

# PPFPL: Cross-silo Privacy-preserving Federated Prototype Learning Against Data Poisoning Attacks on Non-IID Data

Hongliang Zhang, Jiguo Yu, *Fellow, IEEE*, Fenghua Xu, Chunqiang Hu, Yongzhao Zhang, Xiaofen Wang, Zhongyuan Yu, Xiaosong Zhang

**Abstract**—Privacy-Preserving Federated Learning (PPFL) allows multiple clients to collaboratively train by submitting hidden model updates. Nonetheless, PPFL is vulnerable to data poisoning attacks due to the distributed training nature of clients in cross-silo scenarios. Existing solutions have struggled to improve the performance of PPFL in poisoned Non-IID data. To address the issues, this paper proposes a privacy-preserving federated prototype learning framework, named PPFPL, which enhances the cross-silo FL performance in poisoned Non-IID data while protecting the privacy of clients. Specifically, we adopt prototypes as client-submitted model updates to eliminate the impact of poisoned data distribution. In addition, we design a secure aggregation protocol by utilizing homomorphic encryption to achieve Byzantine-robust aggregation on two servers, which greatly reduces the impact of malicious clients. Theoretical analyses confirm the convergence and privacy of PPFPL, and experimental results on publicly datasets show that PPFPL is effective for resisting data poisoning attacks with Non-IID data.

**Index Terms**—Privacy-Preserving, Federated Learning, Cross-Silo, Data Poisoning Attacks, Poisoned Non-IID Data.

## I. INTRODUCTION

Federated Learning (FL) is a distributed learning paradigm where each client shares its model updates instead of raw training data. In industrial applications, massive data is distributed across independent organizations governed by strict

privacy regulations [1]. To break data silos among organizations without compromising privacy, cross-silo FL provides a viable solution for industrial scenarios [2] [3]. Specifically, in cross-silo FL, the clients are usually large organizations, resulting in a relatively small number of clients with significant computational capabilities. However, client-submitted model updates are vulnerable to privacy attacks, which threatens the privacy security of cross-silo FL [4] [5]. To mitigate the privacy risks, Differential Privacy (DP)-based [6] [7] and Homomorphic Encryption (HE)-based [8] [9] PPFL approaches are proposed. In particular, DP-based approach is commonly applied to cross-device FL due to its low computation overhead, but degrades the FL performance by introducing noise. Conversely, HE-based approach offers higher privacy security without sacrificing the global model accuracy, thus making it more suitable for cross-silo FL.

While HE-based approaches demonstrated their effectiveness in terms of privacy preservation, they are susceptible to data poisoning attacks [10] [11]. Specifically, malicious clients launch data poisoning attacks by tampering with their raw training data, and submit model updates derived from the poisoned data, thereby degrading the performance of PPFL [12] [13]. Moreover, privacy-preserving techniques obscure the model updates from malicious clients, making data poisoning attacks more concealed and more difficult to defend. To audit obscured model updates, existing methods [14]–[17] utilize HE and Secure Multi-party Computing (SMC) to identify malicious model updates in ciphertext. However, these works overlook the data heterogeneity in FL, i.e., the data among clients is typically non-independent and identically distributed (Non-IID). The Non-IID data leads to the inconsistency among benign model updates, making it difficult for these defense methods [14]–[17] to distinguish whether the deviations are caused by data heterogeneity or by malicious model updates. To distinguish between benign and malicious updates in the Non-IID data, existing methods [18]–[20] employ clustering or adaptive aggregation weighting operation to mitigate the inconsistency of model updates during the auditing phase, thereby filtering out updates caused by model poisoning attacks. However, in data poisoning attacks, malicious clients tamper with the features and labels of their training data, thereby forming poisoned Non-IID data. These manipulations distort the optimization direction of local training, causing these methods [18]–[20] to optimize toward the tampered Non-IID distribution, thereby degrading

This work was supported by the National Natural Science Foundation of China under Grants 62272256 and 62202250, the Major Program of Shandong Provincial Natural Science Foundation for the Fundamental Research under Grant ZR2022ZD03, the National Science Foundation of Shandong Province under Grant ZR2021QF079, the Colleges and Universities 20 Terms Foundation of Jinan City under Grant 202228093, and the Shandong Province Youth Innovation Team Project under Grant 2024KJH032. (*Corresponding author: Jiguo Yu.*)

H. Zhang is with the School of Computer Science and Technology, Qilu University of Technology, Jinan, 250353, China, Email: b1043123004@stu.qlu.edu.cn.

J. Yu is with School of Computer Science and Engineering, University of Electronic Science and Technology of China, Chengdu, 611731, China, and also with the Big Data Institute, Qilu University of Technology, Jinan, 250353, China, Email: jiguoyu@sina.com; jiguoyu17@uestc.edu.cn.

F. Xu is with the Cyber Security Institute, University of Science and Technology of China, Hefei, 230026, China, Email: nstlxfh@gmail.com.

C. Hu is with the School of Big Data and Software Engineering, Chongqing University, Chongqing, 400044, China, Email: chu@cqu.edu.cn.

Y. Zhang, X. Wang and X. Zhang are with the School of Computer Science and Engineering, University of Electronic Science and Technology of China, Chengdu, 611731, China, Email: zhangyongzhao@uestc.edu.cn, xfwang@uestc.edu.cn, johnsonzxs@uestc.edu.cn.

Z. Yu is with the College of computer science and technology, China University of Petroleum, Qingdao, 266580, China, Email: yuzhy24601@gmail.com.

the performance of FL. Therefore, a critical challenge remains: how to enhance the performance of PPFL in poisoned Non-IID data while effectively resisting data poisoning attacks.

Inspired by prototype learning [21], several works [22]–[25] proposed prototype aggregation to address the Non-IID issue in FL, where prototypes are exchanged between the server and clients. Each prototype represents a class-level feature, computed as the mean of the feature representations of samples belonging to the same class. For instance, the work in [23] suggest that in recognizing the “cat”, different clients have their own unique “imaginary picture” or “prototype” to represent the concept of “cat”. By exchanging these prototypes, clients gain more knowledge about the concept of “cat”. Consequently, prototypes, as feature representations independent of data distribution, inspire our work.

In cases of poisoned Non-IID data, tampered data features and data distribution cannot be repaired since the server cannot control the behavior of malicious clients. This prompts us to pose a question: *Is it possible to design a PPFL that leverages prototype learning, so that client-submitted model updates are affected only by tampered data features but not by tampered data distribution, while incorporating a secure aggregation protocol to eliminate the impact of tampered data features, thereby achieving Byzantine-robust results?* To answer this question, we propose a **Privacy-Preserving Federated Prototype Learning** framework, named PPFPL, which is suitable for cross-silo scenarios. The PPFPL framework consists of two “non-colluding” servers who are “honest but curious” and multiple clients. The key novelty of PPFPL lies in: (i) We propose a novel local optimization function leveraging prototype learning, where each client submit prototypes to two servers, which mitigates the impact of tampered data distributions. (ii) We design a secure aggregation protocol across two servers to aggregate client-submitted prototypes using HE and SMC techniques. This protocol achieves Byzantine-robust results while preventing the privacy of benign clients.

Our main contributions are summarized as follows.

- We are the first to introduce prototype learning into PPFL to defend against data poisoning attacks. By transferring prototypes between clients and servers, our framework mitigates the impact of tampered data distribution and enhances the FL performance in poisoned Non-IID data.
- We utilize HE and SMC techniques to design a secure aggregation protocol across two servers to filter prototypes submitted by malicious clients, ensuring Byzantine-robust results while protecting the privacy of benign clients.
- We provide a convergence guarantee for PPFPL in the presence of data poisoning attacks, which theoretically ensures the framework’s feasibility.
- Compared to existing methods, the superiority of our framework has been empirically validated in poisoned Non-IID data.

The rest of the paper is organized as follows. Section II reviews PPFL works against poisoning attacks. Section III introduces prototype learning and HE. Section IV formalizes the system model. Our PPFPL is detailed in Section V. Section VI provide theoretical analysis. Section VII reviews experimental results. Finally, Section VIII concludes this paper.

## II. RELATED WORK

*Privacy preservation in FL:* Although FL has naturally certain privacy protection, it remains vulnerable to privacy attacks, which causes the privacy threat of benign clients. To resist such attacks, DP-based and HE-based approaches are proposed to preserve client-submitted model updates. Specifically, DP-based schemes [26]–[29] deploy local differential privacy into model updates, ensuring privacy without compromising the utility of model updates. Despite their low computation overheads, these schemes add Gaussian noise or Laplace noise into local model training, which degrades the FL performance to some extent. In contrast, HE is a commonly used cryptographic primitive in across-silo PPFL that provides strong privacy preservation without sacrificing the global model’s accuracy. Specifically, Fang and Qian are one of the first scholars to implement PPFL using HE [30]. They proposed a multi-party machine learning scheme using Paillier [31] technique without compromising clients’ privacy. Considering the heavy communication overhead of Paillier, the work in [32] proposed a privacy-preserving FL using CKKS (i.e., Cheon-Kim-Kim-Song) that reduces computational overhead associated with ciphertexts. This is because CKKS is more efficient and better suitable to handle large-scale vector and multi-parameter network models than Paillier [33]. However, the aforementioned schemes overlook the threat of data poisoning attacks caused by distributed training.

*Resisting data poisoning attacks in FL:* Tolpegin et al. demonstrated that data poisoning attacks can significantly reduce the classification accuracy of the global model, even with a small percentage of malicious clients [34]. Additionally, they proposed an aggregated defense strategy that identifies malicious clients in FL to circumvent data poisoning attacks. Similarly, the works in [35]–[37] proposed detection methods to filter malicious model updates. Differently, Doku et al. employed SVM to audit client’s local training data for excluding malicious clients [38]. However, this work violates the privacy of clients to some extent. Furthermore, the threats of privacy and data poisoning attacks usually coexist in practice across-silo FL. PPFL approaches can utilize cryptographic primitives to provide privacy preservation for clients, while concealing data poisoning attacks from malicious clients.

*Resisting data poisoning attacks in PPFL:* Considering the threats of both privacy and data poisoning attacks, the works such as [14]–[17] combine HE and SMC to identify anomalous model updates in ciphertexts. For instance, the work in [15] proposed a privacy-enhanced FL framework that adopts HE as the underlying technology and provides two servers with a channel to punish malicious clients via gradient extraction of logarithmic function. Similarly, the work in [14] designed a validity checking protocol for ciphertexts under two servers to protect data privacy and adaptively adjust the weight of clients’ gradients to weaken data poisoning attacks. However, these schemes [14]–[17] ignore a fundamental problem, i.e., they neglect the deviations from model updates caused by Non-IID data, making it difficult to distinguish whether the deviations come from malicious model updates or Non-IID data.

To audit malicious updates in PPFL with Non-IID data,

the works in [18] [19] are proposed to eliminate the deviations caused by Non-IID data during the aggregation stage. Specifically, ShieldFL designs a Byzantine-tolerant aggregation mechanism to prevent misjudgments on outliers caused by Non-IID data [18]. Furthermore, Chen et al. adopts clustering combined with cosine similarity and median strategies to eliminate deviations among model updates during aggregation auditing [19]. These schemes can only resist model poisoning attacks confronted by federated learning with Non-IID data, but they cannot essentially improve the performance of FL on Non-IID data. They need to be combined with specialized training techniques designed for Non-IID data (e.g., FedProx [39], FedDyn [40], or FedLC [41], etc.) to radically improve performance of FL. These specialized techniques adds an auxiliary term into local optimization function to constrain model updates of clients, which helps to increase consistency of model updates during local model training. However, in data poisoning attacks, malicious clients tamper with the features and labels of their training data, creating poisoned Non-IID data, which causes specialized training techniques to constrain model updates based on these compromised inputs. Therefore, the above works [18] [19] cannot be combined with the specialized techniques to resist data poisoning attacks while enhancing the FL performance under poisoned Non-IID data.

*Federated prototype learning:* Recently, prototype learning is gradually being applied in federated learning to solve the Non-IID issue. Specifically, the works in [22]–[25] are one of the first to propose federated prototype learning using the concept of prototype learning. Different from the specialized training techniques (e.g., FedProx, FedDyn, or FedLC), the core idea enables clients to pull the same-class samples towards the global prototypes of that class and away from the global prototypes of other classes. In other words, each class holds its corresponding prototype that is independent of other classes. As a result, client-submitted prototype is affected by the samples but is independent of data distribution among clients. This inspires our work: federated prototype learning allows distributed training to remain independent of tampered data distributions caused by data poisoning attacks.

Although prototype learning has already been studied to improve the performance of federated learning in Non-IID data, it has not been explored in privacy-preserving federated learning against data poisoning attacks. Our work is the first to integrate prototype learning into PPFL to tackle the performance degradation caused by tampered Non-IID data in across-silo FL, while preserving the privacy of client-submitted prototypes.

### III. PRELIMINARIES

This section introduces prototypes in federated learning and CKKS technology.

#### A. Prototypes Meet Federated Learning

In the classification task of prototype learning, the prototype is defined as a feature vector representing a specific class [42]. Due to this property, the prototypes of the same class among clients are similar in FL task. Consequently, many FL schemes

[22]–[25] enhance the handling of Non-IID data by prototype learning, which allows clients to align their prototypes with other clients during local model training.

To further understand the prototype calculation in federated prototype learning, we introduce some basic notations below. Let  $\mathcal{S}$  be the set of clients, where each client  $m \in \mathcal{S}$  has an independent private dataset, denoted as  $\mathcal{D}_m = \{(\mathbf{x}_{(i)}, y_{(i)})\}^{|\mathcal{D}_m|}$ . Here,  $|\mathcal{D}_m|$  represents the number of samples in client  $m$ , and  $(\mathbf{x}_{(i)}, y_{(i)})$  denotes sample  $i$  in dataset, where  $\mathbf{x}_{(i)}$  and  $y_{(i)}$  correspond to the feature vector and class label of sample  $i$ , respectively. Meanwhile, let  $\mathcal{I}$  be the set of classes in classification task, where each class  $k$  belongs to  $\mathcal{I}$ . In classification task, the local model includes a feature extractor and a decision classifier. Specifically, the feature extractor transforms sample features into compressed features, while decision classifier maps the compressed features to get classification results. Formally, let  $f_m(\mathbf{r}_{m,t}; \cdot)$  be feature extractor for client  $m$ , parameterized by  $\mathbf{r}_{m,t}$ , where  $t$  denotes the  $t$ -th communication round. Given the feature  $\mathbf{x}_{(i)}$  of sample  $i$ , it is input to feature extractor to obtain compressed feature  $\mathbf{u}_{(i)} = f_m(\mathbf{r}_{m,t}; \mathbf{x}_{(i)})$ . Let  $g_m(\mathbf{z}_{m,t}; \cdot)$  be decision classifier for client  $m$ , parameterized by  $\mathbf{z}_{m,t}$ . The classifier maps the compressed feature  $\mathbf{u}_{(i)}$  to predict the class  $y' = g_m(\mathbf{z}_{m,t}; \mathbf{u}_{(i)})$ . Thus, we denote the local model as  $\mathcal{F}_m((\mathbf{r}_{m,t}, \mathbf{z}_{m,t}); \cdot) = g_m(\mathbf{z}_{m,t}; \cdot) \circ f_m(\mathbf{r}_{m,t}; \cdot)$ , where  $\circ$  denotes composite operator. To simplify notation, we use  $\mathbf{w}_{m,t}$  to denote  $(\mathbf{r}_{m,t}, \mathbf{z}_{m,t})$ , so we have  $\mathcal{F}_m((\mathbf{r}_{m,t}, \mathbf{z}_{m,t}); \cdot) = \mathcal{F}_m(\mathbf{w}_{m,t}; \cdot)$ , and  $\mathbf{w}_{m,t}$  is consider as model parameters for client  $m$ . Next, we introduce calculation process of prototypes.

In federated prototype learning, prototypes can be categorized into local prototypes, computed by clients, and global prototypes, aggregated by the server. Specifically, each client's goal is to align its local prototype to global prototype during local model training. Thus, each client computes its local prototype via its training dataset during local model training. Formally, let  $\mathbf{c}_{m,t}^k$  be the local prototype of class  $k \in \mathcal{I}$  at client  $m$  in  $t$ -th communication round, calculated as

$$\mathbf{c}_{m,t}^k = \frac{1}{|\mathcal{D}_m^k|} \sum_{(\mathbf{x}_{(i)}, y_{(i)}) \in \mathcal{D}_m^k} f_m(\mathbf{r}_{m,t}; \mathbf{x}_{(i)}), \forall k \in \mathcal{I}, \quad (1)$$

where  $\mathcal{D}_m^k$  denotes the dataset with class  $k$  at client  $m$ . The  $\mathbf{c}_{m,t}^k$  can be understood as the mean of compressed features of samples belonging to class  $k$  at client  $m$ . Further, we can get local prototypes for all classes at client  $m$ , denoted as  $\{\mathbf{c}_{m,t}^k\}_{k \in \mathcal{I}}^{|\mathcal{I}|}$ . Once local model training is complete, each client submits its local prototypes to server.

To calculate global prototype, the server adopts an averaging operation to local prototypes submitted by clients. Thus, the global prototype  $\mathbf{C}_{t+1}^k$  for each class is calculated as follows:

$$\mathbf{C}_{t+1}^k = \frac{1}{|\mathcal{S}|} \sum_{m \in \mathcal{S}} \mathbf{c}_{m,t}^k, \forall k \in \mathcal{I}, \quad (2)$$

where  $|\mathcal{S}|$  denotes the number of clients. For global prototypes of all classes, we denote them by the set  $\{\mathbf{C}_{t+1}^k\}_{k \in \mathcal{I}}^{|\mathcal{I}|}$ . Subsequently, the server distributes the latest global prototypes to each client to further train their local model.

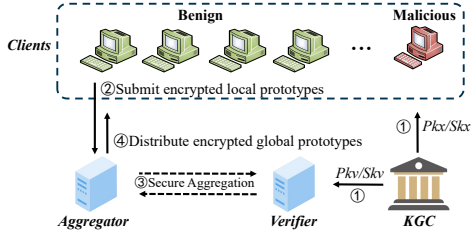


Fig. 1. The PPFPL framework. ① *KGC* generates  $Pk_v/Sk_v$  for *Verifier* and  $Pk_c/Sk_c$  for *Clients*. ② After local training is completed, clients submit encrypted local prototypes to the *Aggregator*. ③ *Verifier* and *Aggregator* perform secure aggregation protocol to get encrypted global prototypes. ④ *Aggregator* distributes encrypted global prototypes to *Clients*.

## B. CKKS

CKKS is a homomorphic encryption technology. Similar to traditional HE, it is a cryptographic technique based on mathematical computations, allowing operations on encrypted data without decrypting. However, traditional HE schemes such as RSA [43], ElGamal [44], and Paillier are limited in that they only support either additive or multiplicative operations but not both simultaneously. In contrast, the CKKS technology provides both additive and multiplicative homomorphic encryption, which is known as full HE [45]. In addition, CKKS is known for its efficiency, especially in terms of encryption/decryption speed when dealing with scale vectors of varying parameter lengths. Therefore, we employ CKKS for the privacy protection of clients due to its computational efficiency. For a more detailed implementation principle and process of CKKS, please refer to paper [46].

## IV. PROBLEM STATEMENT

In the section, we formalize the PPFPL framework, define potential threats, and design goals.

### A. PPFPL framework

The framework of PPFPL consists of four entities, each of which has its specific function, as shown in Fig. 1. The interaction among entities composes operation of whole system. The specific functions of each entity are outlined as follows.

- **Key Generation Center (KGC).** The entity is responsible for generating and managing keys of both *Clients* and *Verifier*, which are important elements to ensure security of encryption/decryption process.
- **Clients.** The *Clients* are large organizations participating in federated training. The aim of benign organizations is to get a better model by federated training. They have a pair of public/secret keys generated by *KGC*, denoted as  $Pk_c/Sk_c$ .
- **Aggregator.** The *Aggregator* is a central server responsible for aggregating local prototypes submitted by clients.
- **Verifier.** The *Verifier* is a non-colluding central server and calculates cooperatively with *Aggregator* to aggregate local prototypes. It has a pair of public/private keys generated by *KGC*, denoted as  $Pk_v/Sk_v$ .

In our framework, we not only define the function of each entity, but also define potential threats.

### B. Potential Threats for PPFPL

We discuss potential threats of PPFPL in detail.

- The *KGC* is a trusted institution (e.g., government, union).
- The *Aggregator* and *Verifier* are considered as “non-colluding” and “curious but honest”. Specifically, we assume that *Aggregator* and *Verifier* do not collude to attack PPFPL. The assumption is reasonable in practice, since it is usually impossible for two well-known service providers to collude with each other due to legal regulations, company reputation [47]. Furthermore, we assume that they follow the system’s protocol but may attempt to get sensitive information (i.e., raw training data) by inferring client-submitted local prototypes. Notably, although prototype is different from gradient, traditional inference attack methods cannot recover client’s private training data from prototype. However, the work in [48] designs a dynamic memory model inversion attack that can recover the private training data by utilizing client’s learned prototypes. Thus, preserving the privacy of prototypes is necessary. In addition, we do not consider security attacks resulting from employee insider threats (e.g., compromised employees within the *Aggregator* or *Verifier*).
- In practice, we cannot guarantee that all clients in the system are honest. Therefore, clients can be either benign or malicious. Specifically, benign clients are “honest but curious”. For malicious clients, they can collude together to infer sensitive information about benign clients. We consider that the proportion of malicious clients is less than 50%, which is a more realistic threat in cross-silo FL due to the high reputation of large organizations participating. Furthermore, malicious clients can launch data poisoning attacks, and submit malicious local prototypes derived from the poisoned data. In federated prototype learning, we define the following two representative types of data poisoning attacks from the perspective of data features and labels.

- **Feature attacks.** The purpose of feature attacks is to degrade the performance of federated learning. Specifically, malicious clients tamper with the features of their training data to generate malicious prototypes for uploading, thereby affecting the training results of other clients.
- **Label attacks.** The malicious clients tamper with the labels of their training samples into other random labels to form the tampered data distribution, aiming to reduce the performance of the entire federated learning.

### C. Design Goals of PPFPL

The goal of our study is to improve performance in cross-silo PPFL under poisoned Non-IID data while resisting data poisoning attacks. Specifically, we design the PPFPL framework to fulfill the following goals:

- **Security.** PPFPL should guarantee the correct model training in the presence of data poisoning attacks with Non-IID data. In other words, the model performance of each benign client is not affected by data poisoning attacks under different data distributions.
- **Privacy.** PPFPL should ensure privacy and security of benign clients. For any third entity, they cannot access the sensitive information about benign clients.

---

**Algorithm 1: Overview of PPFPL**


---

**Input:**  $\mathcal{S}, \mathbf{w}^{init}, E, T$ .  
**Output:** Model parameter of each client.

- 1 Initialize  $T, E, \mathbf{w}^{init}$ ;
- 2 *Aggregator* distributes  $T, E, \mathbf{w}^{init}$  to each client;
- 3 **for** each communication round  $t \in \{1, 2, \dots, T\}$  **do**
- 4    // **Step I: Local Computation.**
- 5    **for** each client  $m \in \mathcal{S}$  **do**
- 6       Train local model;
- 7       Normalize and encrypt local prototypes;
- 8       Send encrypted local prototypes to *Aggregator*;
- 9    // **Step II: Secure Aggregation Protocol.**
- 10    Two servers verify normalization;
- 11    Two servers compute global prototypes;
- 12    *Aggregator* distributes global prototypes to each client;
- 13 **return** Model parameter of each client

---

- **Efficiency.** PPFPL should reduce the number of parameters submitted to two servers compared to other similar frameworks, thereby reducing privacy computation overheads and communication overheads.

## V. DESIGN OF PPFPL

In this section, we first provide the overview of PPFPL, and then describe each step in detail.

### A. Overview of PPFPL

The execution process of PPFPL is summarized in **Algorithm 1**. The framework initializes the number of communication rounds  $T$ , the number of local iterations  $E$ , and the local model's parameters  $\mathbf{w}^{init}$  for each client. Then, *Aggregator*, *Verifier*, and *Clients* jointly perform FL training. Specifically, PPFPL iteratively performs the following two steps:

- *Step I. Local Computation:* Each client trains its local model with its local dataset. Then, the client normalizes and encrypts its local prototypes and submits them to *Aggregator*.
- *Step II. Secure Aggregation Protocol:* The two servers verify the normalization of encrypted local prototypes submitted by clients, and performs the secure two-party computation to get encrypted global prototypes, and distribute them to each client.

The above process is stopped until configured number of communication rounds  $T$ . In the following, we describe the process of *Steps I* and *II* in detail.

### B. Local Computation

The local computation step includes two essential stages: *local model training* and *prototype handling* stages. The detail is outlined in **Algorithm 2**.

1) *Local Model Training:* During local model training, each client aims to minimize classification loss while aligning its local prototype close to the global prototype. To achieve this, we design an auxiliary term by leveraging prototype

---

**Algorithm 2: Local Computation**


---

**Input:**  $\mathcal{S}, \mathcal{D}_m, \eta, \{\llbracket \mathbf{C}_t^k \rrbracket_{P_{kx}}\}_{k \in \mathcal{I}}^{|I|}, E$ .  
**Output:** Encrypted local prototypes.

- 1 **for** each client  $m \in \mathcal{S}$  **do**
- 2    Get global prototypes  $\{\llbracket \mathbf{C}_t^k \rrbracket_{P_{kx}}\}_{k \in \mathcal{I}}^{|I|}$  from *Aggregator*;
- 3    Decrypt  $\{\llbracket \mathbf{C}_t^k \rrbracket_{P_{kx}}\}_{k \in \mathcal{I}}^{|I|}$  using its  $Skx$ ;
- 4     $\mathbf{w}_{m,t}^{(E)} \leftarrow \text{Training}(\mathbf{w}_{m,t-1}^{(E)}, \mathcal{D}_m, \eta, E, \{\mathbf{C}_t^k\}_{k \in \mathcal{I}}^{|I|})$ ;
- 5     $\{\llbracket \mathbf{c}_{m,t}^k \rrbracket_{P_{kv}}\}_{k \in \mathcal{I}}^{|I|} \leftarrow \text{Handling}(\mathbf{w}_{m,t}^{(E)}, \mathcal{D}_m)$ ;
- 6    Send  $\{\llbracket \mathbf{c}_{m,t}^k \rrbracket_{P_{kv}}\}_{k \in \mathcal{I}}^{|I|}$  to *Aggregator*;
- 7 **return**  $\{\llbracket \mathbf{c}_{m,t}^k \rrbracket_{P_{kv}}\}_{k \in \mathcal{I}}^{|I|}$

---

learning in the local optimization function. Formally, the local optimization function of client  $m$  is defined as:

$$\mathcal{L}(\mathbf{w}_m; \mathcal{D}_m, \mathbf{c}_m^k, \mathbf{C}^k) = \mathcal{L}_{\mathcal{S}}(\mathcal{F}_m(\mathbf{w}_m; \mathbf{x}_{(i)}), y_{(i)}) + \lambda \mathcal{L}_{\mathcal{R}}(\mathbf{c}_m^k, \mathbf{C}^k), \forall (\mathbf{x}_{(i)}, y_{(i)}) \in \mathcal{D}_m, \forall k \in \mathcal{I}, \quad (3)$$

where  $\mathcal{L}_{\mathcal{S}}(\cdot, \cdot)$  is the classification loss function (e.g., cross-entropy loss function),  $\lambda$  is the importance weight of auxiliary term, and  $\mathcal{L}_{\mathcal{R}}(\cdot, \cdot)$  is the auxiliary term, defined as

$$\mathcal{L}_{\mathcal{R}}(\mathbf{c}_m^k, \mathbf{C}^k) = \frac{1}{|\mathcal{I}|} \sum_{k \in \mathcal{I}} (1 - \text{sim}(\mathbf{c}_m^k, \mathbf{C}^k)), \quad (4)$$

where  $\text{sim}(\cdot, \cdot)$  denotes cosine similarity between two vectors. The cosine similarity ranges from -1 to 1, where the value closer to “1” indicates similar vector directions, and conversely, the value closer to “-1” means opposing directions. The optimization function ensures that each client reduces the classification loss while aligning its local prototype with the global prototype in direction. Next, we present the process of local model training.

Specifically, in the  $t$ -th communication round, each client  $m$  uses its local dataset  $\mathcal{D}_m$  to iteratively train its local model. This iterative process is executed in **Algorithm 3**. The superscript  $(e)$  indicates the iteration state of variables, where  $e \in \{1, \dots, E\}$ . Each client  $m$  uses its local model parameters  $\mathbf{w}_{m,t-1}^{(E)}$  from the  $(t-1)$ -th round as the starting point in the current  $t$ -th round. Subsequently, each client iteratively performs the following stages.

- In  $e$ -th local iteration, the client randomly selects training data  $\mathcal{D}_m^{(e)}$  from its local dataset  $\mathcal{D}_m$ .
- The client inputs the training data  $\mathcal{D}_m^{(e)}$  into the local model's feature extractor to compute the local prototype  $\mathbf{c}_{m,t}^{k,(e)}$  via formula (1).
- The client computes the unbiased stochastic gradient by

$$\mathbf{g}_{m,t}^{(e-1)} = \nabla \mathcal{L}(\mathbf{w}_{m,t}^{(e-1)}; \mathcal{D}_m^{(e)}, \mathbf{c}_{m,t}^{k,(e)}, \mathbf{C}_t^k),$$

where  $\nabla$  denotes derivation operation. Then, the local model  $\mathbf{w}_{m,t}^{(e-1)}$  is updated via the following formula:

$$\mathbf{w}_{m,t}^{(e)} = \mathbf{w}_{m,t}^{(e-1)} - \eta \mathbf{g}_{m,t}^{(e-1)},$$

where  $\eta$  is the local learning rate.

After  $E$  local iterations of the above process, each client derives the updated local model parameters  $\mathbf{w}_{m,t}^{(E)}$ .

---

**Algorithm 3: Training**


---

**Input:**  $\mathbf{w}_{m,t-1}^{(E)}$ ,  $\mathcal{D}_m$ ,  $\eta$ ,  $E$ ,  $\{\mathbf{C}_t^k\}_{k \in \mathcal{I}}^{|I|}$ .  
**Output:** Local model parameters of each client  $\mathbf{w}_{m,t}^{(E)}$ .

```

1  $\mathbf{w}_{m,t}^{(0)} = \mathbf{w}_{m,t-1}^{(E)}$ ;
2 for each local iteration  $e \in \{1, 2, \dots, E\}$  do
3   Randomly sample  $\mathcal{D}_m^{(e)} \subset \mathcal{D}_m$ ;
4   for each class  $k \in \mathcal{I}$  do
5     Calculate  $\mathbf{c}_{m,t}^{k,(e)}$  from  $\mathcal{D}_m^{k,(e)}$  with formula (1);
6    $\mathbf{g}_{m,t}^{(e-1)} = \nabla \mathcal{L}(\mathbf{w}_{m,t}^{(e-1)}; \mathcal{D}_m^{(e)}, \mathbf{c}_{m,t}^{k,(e)}, \mathbf{C}_t^k)$ ;
7    $\mathbf{w}_{m,t}^{(e)} = \mathbf{w}_{m,t}^{(e-1)} - \eta \mathbf{g}_{m,t}^{(e-1)}$ ;
8 return  $\mathbf{w}_{m,t}^{(E)}$ 

```

---



---

**Algorithm 4: Handling**


---

**Input:**  $\mathbf{r}_{m,t}^{(E)}$ ,  $\mathcal{D}_m$   
**Output:**  $\{\llbracket \mathbf{c}_{m,t}^k \rrbracket\}_{k \in \mathcal{I}}^{|I|}$

```

1 for each class  $k \in \mathcal{I}$  do
2    $\mathbf{c}_{m,t}^k = \frac{1}{|\mathcal{D}_m^k|} \sum_{(\mathbf{x}_{(i)}, y_{(i)}) \in \mathcal{D}_m^k} f_m(\mathbf{r}_{m,t}^{(E)}; \mathbf{x}_{(i)})$ ;
3    $\tilde{\mathbf{c}}_m^k = \mathbf{c}_{m,t}^k / \|\mathbf{c}_{m,t}^k\|$ ;
4   Encrypt  $\tilde{\mathbf{c}}_m^k$  by Verifier's  $P_{kv}$  to get  $\llbracket \tilde{\mathbf{c}}_m^k \rrbracket_{P_{kv}}$ ;
5 return  $\{\llbracket \mathbf{c}_{m,t}^k \rrbracket\}_{k \in \mathcal{I}}^{|I|}$ 

```

---

2) *Prototype Handling*: The prototype handling stage consists of three key phases: *prototype generation*, *normalization*, and *encryption*, as illustrated in **Algorithm 4**.

a) *Prototype Generation*: Since the parameters of local model change with each iteration, the prototypes generated by each local iteration are different. Consequently, the local prototypes evolve dynamically during local model training. To submit more representative prototypes, each client regenerates them via the local model parameters  $\mathbf{w}_{m,t}^{(E)}$ . Formally, let  $\mathbf{c}_{m,t}^k$  be the submitted local prototype, is computed as:

$$\mathbf{c}_{m,t}^k = \frac{1}{|\mathcal{D}_m^k|} \sum_{(\mathbf{x}_{(i)}, y_{(i)}) \in \mathcal{D}_m^k} f_m(\mathbf{r}_{m,t}^{(E)}; \mathbf{x}_{(i)}), \forall k \in \mathcal{I},$$

where  $\mathbf{r}_{m,t}^{(E)}$  is the parameters of feature extractor.

b) *Normalization*: Considering that malicious clients amplify their submitted local prototypes, the local prototype of each class in each client is normalized. Formally, the local prototype is normalized by the following formula:

$$\tilde{\mathbf{c}}_{m,t}^k = \mathbf{c}_{m,t}^k / \|\mathbf{c}_{m,t}^k\|, \forall m \in \mathcal{S}, k \in \mathcal{I},$$

where  $\tilde{\mathbf{c}}_{m,t}^k$  is a unit vector. After normalization, each local prototype needs to be encrypted for privacy protection.

c) *Encryption*: To protect privacy of clients, they encrypts their own normalized local prototypes  $\tilde{\mathbf{c}}_{m,t}^k$  using the Verifier's public key  $P_{kv}$  to get  $\llbracket \tilde{\mathbf{c}}_{m,t}^k \rrbracket_{P_{kv}}$ , and sends the  $\{\llbracket \tilde{\mathbf{c}}_{m,t}^k \rrbracket_{P_{kv}}\}_{k \in \mathcal{I}}^{|I|}$  to Aggregator, where CKKS technique is used to encrypt.

### C. Secure Aggregation

To resist local prototypes submitted by malicious clients without compromising privacy, we design a secure aggregation

protocol across two servers to filter malicious local prototypes and obtain Byzantine-robust global prototypes. The protocol consists of *normalization verification* and *secure two-party computation*.

1) *Normalization verification*: Since malicious clients may bypass the normalization stage to amplify the impact of their local prototypes, the two servers need to verify that encrypted local prototypes are normalized. Specifically, Aggregator calculates the inner product  $\llbracket \tilde{\mathbf{c}}_{m,t}^k \rrbracket_{P_{kv}} \cdot \llbracket \tilde{\mathbf{c}}_{m,t}^k \rrbracket_{P_{kv}}$  for each local prototype, and sends the results to Verifier, where  $\cdot$  denotes the inner product. Then, the Verifier decrypts  $\llbracket \tilde{\mathbf{c}}_{m,t}^k \rrbracket_{P_{kv}} \cdot \llbracket \tilde{\mathbf{c}}_{m,t}^k \rrbracket_{P_{kv}}$  using its secret key  $Skv$ , and checks whether the inner product  $\|\tilde{\mathbf{c}}_{m,t}^k\|^2$  equals 1. If the inner product of prototype from client  $m$  is not equal to 1, which indicates that its local prototype does not normalized, client  $m$  is removed from the set of clients  $\mathcal{S}$ . After validation, Verifier sends the remaining client set  $\mathcal{S}$  to Aggregator.

2) *Secure Two-party Computation*: To achieve privacy preservation and Byzantine-robust aggregation results, two servers perform secure two-party computation to calculate global prototypes. The computing of global prototype is shown in **Algorithm 5** and described as follows.

---

**Algorithm 5: SecComput**


---

**Input:**  $\llbracket \tilde{\mathbf{c}}_{m,t}^k \rrbracket_{P_{kv}}$ ,  $\mathcal{S}$ ,  $\chi$ .  
**Output:**  $\llbracket \mathbf{C}_{t+1}^k \rrbracket_{P_{kx}}$ .

```

1 Aggregator:
2   Compute trusted prototype  $\llbracket \mathbf{C}_{t+1}^k \rrbracket_{P_{kv}}$  by formula (5);
3   Compute  $\llbracket \text{sim}_{m,t}^k \rrbracket_{P_{kv}}$  by formula (6);
4   Compute  $\llbracket \text{sim}_{m,t}^k \rrbracket_{P_{kv}}$  and  $\llbracket \chi' \rrbracket_{P_{kv}}$ ;
5    $\llbracket h_{m,t}^k \rrbracket_{P_{kv}} \leftarrow \text{OutPut}(\llbracket \text{sim}_{m,t}^k \rrbracket_{P_{kv}}, \llbracket \chi' \rrbracket_{P_{kv}})$ ;
6   Randomly select a  $n$ -dimensional vector  $\mathbf{V}^n$  and a number  $p$ ;
7   Send  $p \times \llbracket h_{m,t}^k \rrbracket_{P_{kv}}$  and  $\mathbf{V}^n \odot \llbracket \tilde{\mathbf{c}}_{m,t}^k \rrbracket_{P_{kv}}$  to Verifier;
8 Verifier:
9   Decrypt  $p \times \llbracket h_{m,t}^k \rrbracket_{P_{kv}}$  and  $\mathbf{V}^n \odot \llbracket \tilde{\mathbf{c}}_{m,t}^k \rrbracket_{P_{kv}}$  with  $Skv$ ;
10  Compute  $j_{m,t}^k$  by formula (8);
11  Compute  $\text{Sum}_t^k$ ;
12  Encrypt  $j_{m,t}^k$ ,  $\mathbf{V}^n \odot \tilde{\mathbf{c}}_{m,t}^k$  using Clients'  $P_{kx}$ ;
13  Send  $\text{Sum}_t^k$ ,  $\llbracket j_{m,t}^k \rrbracket_{P_{kx}}$ , and  $\llbracket \mathbf{V}^n \odot \tilde{\mathbf{c}}_{m,t}^k \rrbracket_{P_{kx}}$  to Aggregator;
14 Aggregator:
15  Compute  $\llbracket \tilde{\mathbf{c}}_{m,t}^k \rrbracket_{P_{kx}} \leftarrow \frac{1}{V^n} \odot \llbracket \mathbf{V}^n \odot \tilde{\mathbf{c}}_{m,t}^k \rrbracket_{P_{kx}}$ ;
16  Aggregate global prototype  $\llbracket \mathbf{C}_{t+1}^k \rrbracket_{P_{kx}}$  by formula (9);
17  Distribute global prototype  $\llbracket \mathbf{C}_{t+1}^k \rrbracket_{P_{kx}}$  to clients;

```

---

Specifically, malicious clients exploit poisoned local data to generate local prototypes with low credibility. Conversely, local prototypes submitted by benign clients should have high credibility. However, for each class without a trusted prototype direction, it is difficult to assess the credibility of submitted prototypes. To this end, Aggregator computes the trusted prototype via the formula:

$$\llbracket \mathbf{C}_{t+1}^k \rrbracket_{P_{kv}} = \frac{1}{|\mathcal{S}|} \sum_{m \in \mathcal{S}} \llbracket \mathbf{c}_{m,t}^k \rrbracket_{P_{kv}}, \forall k \in \mathcal{I}, \quad (5)$$

where  $\llbracket \mathbf{C}_{t+1}^k \rrbracket_{P_{kv}}$  denotes the trusted prototype for class  $k$  in  $(t+1)$ -th communication round.  $\mathbf{C}_{t+1}^k$  is considered a

trusted prototype for two reasons: 1) In terms of magnitude, this is because the normalized malicious prototype do not affect the magnitude of trusted prototype, only the direction of trusted prototype; 2) In terms of direction, the average of all prototypes remains a plausible direction due to the small proportion of malicious clients. Subsequently, *Aggregator* obtains the plaintext  $\llbracket \mathbf{C}_{t+1}^k \rrbracket$  for subsequent cosine similarity computation. To achieve the plaintext, it computes the inner product  $\llbracket \mathbf{C}_{t+1}^k \rrbracket_{Pkv} \cdot \llbracket \mathbf{C}_{t+1}^k \rrbracket_{Pkv}$  and sends it to the *Verifier* for decryption, then receives the decrypted result. Then, cosine similarity, a widely used measure of the angle between two vectors, is employed to measure the credibility of local prototype. If the direction of local prototype is similar to that of trusted prototype, its credibility is higher. Formally, *Aggregator* computes the credibility of local prototype by the following formula,

$$\begin{aligned} \llbracket \text{sim}_{m,t}^k \rrbracket_{Pkv} &= \llbracket \text{sim}(\tilde{\mathbf{c}}_{m,t}^k, \mathbf{C}_{t+1}^k) \rrbracket_{Pkv} = \left\llbracket \frac{\tilde{\mathbf{c}}_{m,t}^k \cdot \mathbf{C}_{t+1}^k}{\|\tilde{\mathbf{c}}_{m,t}^k\| \|\mathbf{C}_{t+1}^k\|} \right\rrbracket_{Pkv} \\ &= \frac{1}{\|\mathbf{C}_{t+1}^k\|} \left( \llbracket \tilde{\mathbf{c}}_{m,t}^k \rrbracket_{Pkv} \cdot \llbracket \mathbf{C}_{t+1}^k \rrbracket_{Pkv} \right), \end{aligned} \quad (6)$$

where  $\llbracket \text{sim}_{m,t}^k \rrbracket_{Pkv}$  denotes the credibility of local prototype. Additionally, we set the detection threshold  $\chi$  and define local prototypes with its credibility less than  $\chi$  as anomalous local prototypes. During global prototype aggregation, we set the aggregation weight of anomalous local prototype to 0. Formally, the aggregation weight of each local prototype is calculated as follows:

$$j_{m,t}^k = \begin{cases} 0, & \text{sim}_{m,t}^k < \chi \\ \llbracket \text{sim}_{m,t}^k \rrbracket_{Pkv}, & \text{sim}_{m,t}^k > \chi, \end{cases} \quad (7)$$

where  $j_{m,t}^k$  denotes the aggregation weight of local prototype for class  $k$  at client  $m$  in the  $t$ -th communication round. However, *Aggregator* cannot directly compare  $\llbracket \text{sim}_{m,t}^k \rrbracket_{Pkv}$  with  $\chi$  under encryption domain.

To implement comparison within encryption domain, the work in [49] offers a ciphertext comparison method that outputs the maximum value of homomorphic ciphertexts corresponding to two plaintexts in the range (0, 1) without decryption. However, since the cosine similarity ranges from -1 to 1, and the method cannot be applied directly. To resolve the range mismatch, *Aggregator* sets  $\llbracket \text{sim}_{m,t}^k \rrbracket = \frac{1}{2}(\llbracket \text{sim}_{m,t}^k \rrbracket + \llbracket 1 \rrbracket)$  and  $\chi' = \frac{1}{2}(\chi + 1)$  as input to the comparison method [49]. This is because the size relationship between  $\llbracket \text{sim}_{m,t}^k \rrbracket$  and  $\chi$  remains unchanged. Then, *Aggregator* encrypts  $\chi'$  to get  $\llbracket \chi' \rrbracket$ , and calculates the maximum value  $\llbracket h_{m,t}^k \rrbracket$  between  $\llbracket \text{sim}_{m,t}^k \rrbracket$  and  $\llbracket \chi' \rrbracket$  by **Algorithm 6**.

After obtaining the maximum value  $\llbracket h_{m,t}^k \rrbracket_{Pkv}$ , *Aggregator* collaborates with *Verifier* to calculate the aggregation results. Specifically, *Aggregator* selects a random value  $p$ , and multiplies it by the maximum value to get  $p \times \llbracket h_{m,t}^k \rrbracket_{Pkv}$ . Additionally, *Aggregator* chooses a random vector  $\mathbf{V}$  with the same dimension as the prototype, and computes its hadamard product with local prototype to obtain  $\mathbf{V} \odot \llbracket \tilde{\mathbf{c}}_{m,t}^k \rrbracket_{Pkv}$ , where  $\odot$  denotes the hadamard product. Then, *Aggregator* sends  $p \times \llbracket h_{m,t}^k \rrbracket_{Pkv}$  and  $\mathbf{V} \odot \llbracket \tilde{\mathbf{c}}_{m,t}^k \rrbracket_{Pkv}$  to *Verifier*. The *Verifier* then

#### Algorithm 6: OutPut

---

**Input:**  $(\llbracket \text{sim}_{m,t}^k \rrbracket, \llbracket \chi' \rrbracket) \in (\llbracket 0 \rrbracket, \llbracket 1 \rrbracket), d \in \mathbb{N}$   
**Output:** an max value of  $\llbracket \text{sim}_{m,t}^k \rrbracket$  or  $\llbracket \chi' \rrbracket$

---

```

1  $a = \llbracket \text{sim}_{m,t}^k \rrbracket, b = \llbracket \chi' \rrbracket;$ 
2  $q_1 = \frac{(a+b)}{2}, q_2 = \frac{(a-b)}{2};$ 
3  $a_0 = q_2^2, b_0 = q_2^2 - 1;$ 
4 for each  $n \in (0, d-1)$  do
5    $a_{n+1} = a_n(1 - \frac{b_n}{2});$ 
6    $b_{n+1} = b_n^2(\frac{b_n-3}{4});$ 
7  $q_3 = a_d;$ 
8 return  $(q_1 + q_3)$ 
```

---

decrypts these values by its secret key  $Skv$  to get  $p \times h_{m,t}^k$  and  $\mathbf{V} \odot \tilde{\mathbf{c}}_{m,t}^k$ . Since the random value  $p$  and random vector  $\mathbf{V}$  obfuscate  $h_{m,t}^k$  and  $\llbracket \tilde{\mathbf{c}}_{m,t}^k \rrbracket_{Pkv}$ , respectively, *Verifier* cannot extract sensitive information about clients from  $p \times h_{m,t}^k$  and  $\mathbf{V} \odot \tilde{\mathbf{c}}_{m,t}^k$ . Then, the aggregation weight is rewritten as the following formula:

$$j_{m,t}^k = \begin{cases} 0, & \text{Round}(p \times h_{m,t}^k, 6) = \min_t^k \\ p \times h_{m,t}^k, & \text{Round}(p \times h_{m,t}^k, 6) > \min_t^k, \end{cases} \quad (8)$$

where  $\text{Round}(p \times h_{m,t}^k, 6)$  denotes that  $p \times h_{m,t}^k$  is rounded to the 6-th decimal place. This is because CKKS decrypts the ciphertext with an error in the range of  $10^{-7}$  [50]. Moreover,  $\min_t^k$  denotes the smallest value for class  $k$  in set  $\{\text{Round}(p \times h_{m,t}^k, 6)\}_{m \in \mathcal{S}}^{|S|}$ . The  $\text{Round}(p \times h_{m,t}^k, 6) = \min_t^k$  means that the local prototype  $\tilde{\mathbf{c}}_{m,t}^k$  satisfies  $\text{sim}_{m,t}^k < \chi$ , thus its aggregation weight  $j_{m,t}^k$  is 0. Additionally, *Verifier* calculates  $\text{Sum}_t^k = \sum_{m \in \mathcal{S}} j_{m,t}^k$  and encrypts  $j_{m,t}^k$  and  $\mathbf{V} \odot \tilde{\mathbf{c}}_{m,t}^k$  using the client's public key  $Pkx$  to get  $\llbracket j_{m,t}^k \rrbracket_{Pkx}$  and  $\llbracket \mathbf{V} \odot \tilde{\mathbf{c}}_{m,t}^k \rrbracket_{Pkx}$ , and sends them to *Aggregator*.

The *Aggregator* computes  $\frac{1}{V} \odot \llbracket \mathbf{V} \odot \tilde{\mathbf{c}}_{m,t}^k \rrbracket_{Pkx}$  to get  $\llbracket \tilde{\mathbf{c}}_{m,t}^k \rrbracket_{Pkx}$ , and aggregates the encrypted local prototypes to get the encrypted global prototype  $\llbracket \mathbf{C}_{t+1}^k \rrbracket_{Pkx}$  by the following formula,

$$\llbracket \mathbf{C}_{t+1}^k \rrbracket_{Pkx} = \frac{1}{\text{Sum}_t^k} \sum_{m \in \mathcal{S}} \llbracket j_{m,t}^k \rrbracket_{Pkx} \times \llbracket \tilde{\mathbf{c}}_{m,t}^k \rrbracket_{Pkx}. \quad (9)$$

Subsequently, the *Aggregator* distributes the encrypted global prototype to *Clients*. After the above process is completed, FL executes the next communication round until a predefined number of rounds is reached.

## VI. ANALYSIS

In the section, we provide both convergence analysis and privacy analysis for PPFPL. Specifically, we make the following assumptions similar to existing general frameworks [22] [51] for loss function (3).

**Assumption 1.** Each loss function is  $L_1$  Lipschitz smooth, which means that the gradient of loss function is  $L_1$  Lipschitz continuous, we can get

$$\left\| \nabla \mathcal{L}_{m,t}^{(e_1)} - \nabla \mathcal{L}_{m,t}^{(e_2)} \right\|_2 \leq L_1 \left\| \mathbf{w}_{m,t}^{(e_1)} - \mathbf{w}_{m,t}^{(e_2)} \right\|_2,$$



where  $\mathcal{L}_{m,t}^{(e_1)}$  denotes loss function at the  $(tE + e_1)$ -th local iteration in client  $m$ . This implies the following quadratic bound,

$$\begin{aligned} \mathcal{L}_{m,t}^{(e_1)} - \mathcal{L}_{m,t}^{(e_2)} &\leq \left\langle \nabla \mathcal{L}_{m,t}^{(e_2)}, \left( \mathbf{w}_{m,t}^{(e_1)} - \mathbf{w}_{m,t}^{(e_2)} \right) \right\rangle + \frac{L_1}{2} \left\| \mathbf{w}_{m,t}^{(e_1)} - \mathbf{w}_{m,t}^{(e_2)} \right\|_2^2. \end{aligned}$$

**Assumption 2.** The stochastic gradient  $\mathbf{g}_{m,t}^{(e)} = \nabla \mathcal{L}(\mathbf{w}_{m,t}^{(e-1)}; \mathcal{D}_m^{(e)})$  is an unbiased estimator of the local gradient for each client. Suppose its expectation

$$\mathbb{E}_{\mathcal{D}_m^{(e)} \sim \mathcal{D}_m} [\mathbf{g}_{m,t}^{(e)}] = \nabla \mathcal{L}(\mathbf{w}_{m,t}^{(e)}; \mathcal{D}_m^{(e)}) = \nabla \mathcal{L}_{m,t}^{(e)},$$

and its variance is bounded by  $\sigma^2$ :

$$\mathbb{E}[\|\mathbf{g}_{m,t}^{(e)} - \nabla \mathcal{L}(\mathbf{w}_{m,t}^{(e)})\|_2^2] \leq \sigma^2.$$

Based on the above assumptions, we have the following theorem and corollaries. Notably, we add “ $\frac{1}{2}$ ” into the local iteration, denoted as  $\{\frac{1}{2}, 1, \dots, E\}$  in our analysis. For example,  $tE$  denotes the time step before local prototype aggregation, and  $tE + \frac{1}{2}$  denotes the time step between local prototype aggregation and the first local iteration of the  $t$ -th round.

**Theorem 1.** In PPFPL, regardless of the percentage of malicious clients, for the  $t$ -th communication round, the variation of loss function for each benign client can be bounded as,

$$\mathbb{E}[\mathcal{L}_{m,t+\frac{1}{2}}^{\frac{1}{2}}] - \mathcal{L}_{m,t}^E \leq G(\lambda, \eta, E),$$

where

$$G(\lambda, \eta, E) = -\left(\eta - \frac{\eta^2 L_1}{2}\right) \sum_{e=\frac{1}{2}}^E \left\| \nabla \mathcal{L}_{m,t}^{(e)} \right\|_2^2 + \frac{E\eta^2 L_1}{2} \sigma^2 + 2\lambda.$$

*Proof.* Assuming that **Assumption 1** holds, we can get

$$\begin{aligned} \mathcal{L}_{m,t}^{(1)} &\leq \mathcal{L}_{m,t}^{(\frac{1}{2})} + \left\langle \nabla \mathcal{L}_{m,t}^{(\frac{1}{2})}, \left( \mathbf{w}_{m,t}^{(1)} - \mathbf{w}_{m,t}^{(\frac{1}{2})} \right) \right\rangle + \frac{L_1}{2} \left\| \mathbf{w}_{m,t}^{(1)} - \mathbf{w}_{m,t}^{(\frac{1}{2})} \right\|_2^2 \\ &\stackrel{(a)}{=} \mathcal{L}_{m,t}^{(\frac{1}{2})} - \eta \left\langle \nabla \mathcal{L}_{m,t}^{(\frac{1}{2})}, \mathbf{g}_{m,t}^{(\frac{1}{2})} \right\rangle + \frac{\eta^2 L_1}{2} \left\| \mathbf{g}_{m,t}^{(\frac{1}{2})} \right\|_2^2, \end{aligned} \quad (10)$$

where (a) follows from  $\mathbf{w}_{m,t}^{(1)} = \mathbf{w}_{m,t}^{(\frac{1}{2})} - \eta \mathbf{g}_{m,t}^{(\frac{1}{2})}$ . Taking expectation on both sides of formula (10), we can get

$$\begin{aligned} \mathbb{E}[\mathcal{L}_{m,t}^{(1)}] &\leq \mathcal{L}_{m,t}^{(\frac{1}{2})} - \eta \mathbb{E} \left[ \left\langle \nabla \mathcal{L}_{m,t}^{(\frac{1}{2})}, \mathbf{g}_{m,t}^{(\frac{1}{2})} \right\rangle \right] + \frac{\eta^2 L_1}{2} \mathbb{E} \left[ \left\| \mathbf{g}_{m,t}^{(\frac{1}{2})} \right\|_2^2 \right] \\ &\stackrel{(b)}{=} \mathcal{L}_{m,t}^{(\frac{1}{2})} - \eta \left\| \nabla \mathcal{L}_{m,t}^{(\frac{1}{2})} \right\|_2^2 + \frac{\eta^2 L_1}{2} \mathbb{E} \left[ \left\| \mathbf{g}_{m,t}^{(\frac{1}{2})} \right\|_2^2 \right] \\ &\stackrel{(c)}{=} \mathcal{L}_{m,t}^{(\frac{1}{2})} - \eta \left\| \nabla \mathcal{L}_{m,t}^{(\frac{1}{2})} \right\|_2^2 + \frac{\eta^2 L_1}{2} \left( \mathbb{E}[\|\mathbf{g}_{m,t}^{(\frac{1}{2})}\|_2^2] + \text{Var}(\mathbf{g}_{m,t}^{(\frac{1}{2})}) \right) \\ &\stackrel{(d)}{\leq} \mathcal{L}_{m,t}^{(\frac{1}{2})} - \eta \left\| \nabla \mathcal{L}_{m,t}^{(\frac{1}{2})} \right\|_2^2 + \frac{\eta^2 L_1}{2} \left( \left\| \nabla \mathcal{L}_{m,t}^{(\frac{1}{2})} \right\|_2^2 + \text{Var}(\mathbf{g}_{m,t}^{(\frac{1}{2})}) \right) \\ &= \mathcal{L}_{m,t}^{(\frac{1}{2})} - \left( \eta - \frac{\eta^2 L_1}{2} \right) \left\| \nabla \mathcal{L}_{m,t}^{(\frac{1}{2})} \right\|_2^2 + \frac{\eta^2 L_1}{2} \text{Var}(\mathbf{g}_{m,t}^{(\frac{1}{2})}) \\ &\stackrel{(e)}{\leq} \mathcal{L}_{m,t}^{(\frac{1}{2})} - \left( \eta - \frac{\eta^2 L_1}{2} \right) \left\| \nabla \mathcal{L}_{m,t}^{(\frac{1}{2})} \right\|_2^2 + \frac{\eta^2 L_1}{2} \sigma^2, \end{aligned}$$

where (b), (d) and (e) follow from **Assumption 2**, (c) follows from  $\text{Var}(x) = \mathbb{E}[x^2] - (\mathbb{E}[x])^2$ . Then, during the local computation step, the loss function is updated  $E$  times, and it can be bounded as:

$$\mathbb{E}[\mathcal{L}_{m,t}^{(1)}] \leq \mathcal{L}_{m,t}^{(\frac{1}{2})} - \left( \eta - \frac{\eta^2 L_1}{2} \right) \sum_{e=\frac{1}{2}}^E \left\| \nabla \mathcal{L}_{m,t}^{(e)} \right\|_2^2 + \frac{E\eta^2 L_1}{2} \sigma^2. \quad (11)$$

Additionally, since a single communication round involves both local computation and secure aggregation, we need to compute the impact of the aggregation result for loss function of each benign client. Specifically, the loss function of each benign client at the  $((t+1)E + \frac{1}{2})$  time step is represented as follows:

$$\begin{aligned} \mathcal{L}_{m,t+\frac{1}{2}}^{\frac{1}{2}} &= \mathcal{L}_{m,t}^E + \mathcal{L}_{m,t+\frac{1}{2}}^{\frac{1}{2}} - \mathcal{L}_{m,t}^E \\ &= \mathcal{L}_{m,t}^E + \lambda \mathcal{L}_{\mathcal{R}}(\mathbf{c}_{m,t+\frac{1}{2}}^k, \mathbf{C}_{t+\frac{1}{2}}^k) - \lambda \mathcal{L}_{\mathcal{R}}(\mathbf{c}_{m,t+\frac{1}{2}}^k, \mathbf{C}_{t+\frac{1}{2}}^k) \\ &= \mathcal{L}_{m,t}^E - \frac{\lambda}{|\mathcal{I}|} \sum_{k \in \mathcal{I}} \text{sim}(\mathbf{c}_{m,t+\frac{1}{2}}^k, \mathbf{C}_{t+\frac{1}{2}}^k) + \frac{\lambda}{|\mathcal{I}|} \sum_{k \in \mathcal{I}} \text{sim}(\mathbf{c}_{m,t+\frac{1}{2}}^k, \mathbf{C}_{t+\frac{1}{2}}^k) \\ &\stackrel{(f)}{\leq} \mathcal{L}_{m,t}^E + 2\lambda, \end{aligned} \quad (12)$$

where (f) follows from  $-1 \leq \text{sim}(\cdot, \cdot) \leq 1$ . Taking expectation on both sides of formula (12), we can get

$$\mathbb{E}[\mathcal{L}_{m,t+\frac{1}{2}}^{\frac{1}{2}}] \leq \mathcal{L}_{m,t}^E + 2\lambda. \quad (13)$$

Thus, during the  $t$ -th communication round, according to the formula (11) and formula (13), the variation of loss function for each benign client can be bounded as,

$$\mathbb{E}[\mathcal{L}_{m,t+\frac{1}{2}}^{\frac{1}{2}}] - \mathcal{L}_{m,t}^E \leq G(\lambda, \eta, E),$$

where

$$G(\lambda, \eta, E) = -\left(\eta - \frac{\eta^2 L_1}{2}\right) \sum_{e=\frac{1}{2}}^E \left\| \nabla \mathcal{L}_{m,t}^{(e)} \right\|_2^2 + \frac{E\eta^2 L_1}{2} \sigma^2 + 2\lambda.$$

Thus, **Theorem 1** is proved.  $\square$

**Corollary 1.** Given any fixed  $\lambda$  and  $E$ , the  $G(\eta)$  is a convex function with respect to  $\eta$ .

*Proof.* To prove that  $G(\eta)$  is a convex function for  $\eta$ , we need to prove that the second order derivative of  $G(\eta)$  with respect to  $\eta$  is always nonnegative. Thus, we have

$$\frac{dG(\eta)}{d\eta} = -(1 - L_1\eta) \sum_{e=\frac{1}{2}}^E \left\| \nabla \mathcal{L}_{m,t}^{(e)} \right\|_2^2 + L_1 E \eta \sigma^2,$$

and

$$\frac{d^2 G(\eta)}{d\eta^2} = L_1 \sum_{e=\frac{1}{2}}^E \left\| \nabla \mathcal{L}_{m,t}^{(e)} \right\|_2^2 + L_1 E \sigma^2.$$

Since  $L_1$ ,  $E$ , and  $\sigma^2$  are all greater than 0, we have  $\frac{d^2 G(\eta)}{d\eta^2} > 0$ . Thus,  $G(\eta)$  is proved to be a convex function and there exists a minimum value of  $G(\eta)$ .  $\square$



**Corollary 2.** *Given any fixed  $\lambda$  and  $E$ , the variation of the loss function compared to the previous round exists a minimum*

$$\text{bound when } \eta = \eta^*, \text{ where } \eta^* = \frac{\sum_{e=\frac{1}{2}}^E \|\nabla \mathcal{L}_{m,t}^{(e)}\|_2^2}{L_1 E \sigma^2 + L_1 \sum_{e=\frac{1}{2}}^E \|\nabla \mathcal{L}_{m,t}^{(e)}\|_2^2}.$$

*Proof.* When  $G'(\eta)$  equals 0, then  $G(\eta)$  obtains a extremum value. Let  $(\frac{dG(\eta)}{d\eta}|_{\eta=\eta^*}) = 0$ , so we get

$$(\frac{dG(\eta)}{d\eta}|_{\eta=\eta^*}) = -(1 - L_1 \eta) \sum_{e=\frac{1}{2}}^E \|\nabla \mathcal{L}_{m,t}^{(e)}\|_2^2 + L_1 E \eta \sigma^2 = 0.$$

Thus,  $G(\eta)$  exists a extremum value when  $\eta = \eta^* = \frac{\sum_{e=\frac{1}{2}}^E \|\nabla \mathcal{L}_{m,t}^{(e)}\|_2^2}{L_1 E \sigma^2 + L_1 \sum_{e=\frac{1}{2}}^E \|\nabla \mathcal{L}_{m,t}^{(e)}\|_2^2}$ . Because corollary 1 proves the second order derivative of  $G(\eta)$  with respect to  $\eta$  is always non-negative, the extremum value is the minimal value. Therefore, we can understand that the variation of loss function exists a minimum bound when  $\eta = \eta^*$ .  $\square$

**Corollary 3.** *Given any fixed  $\eta$  and  $E$ , the loss function of arbitrary client monotonously decreases in each communication round when  $\lambda < (\frac{1}{2}\eta - \frac{L_1 \eta^2}{4}) \sum_{e=\frac{1}{2}}^E \|\nabla \mathcal{L}_{m,t}^{(e)}\|_2^2 - \frac{E \eta^2 L_1}{4} \sigma^2$ .*

*Proof.* To guarantee that the local loss function decreases after each communication, we need to make sure that  $G(\lambda) < 0$ , so we have

$$-\left(\eta - \frac{L_1 \eta^2}{2}\right) \sum_{e=\frac{1}{2}}^E \|\nabla \mathcal{L}_{m,t}^{(e)}\|_2^2 + \frac{E \eta^2 L_1}{2} \sigma^2 + 2\lambda < 0.$$

After simplification, we get

$$\lambda < \left(\frac{1}{2}\eta - \frac{L_1 \eta^2}{4}\right) \sum_{e=\frac{1}{2}}^E \|\nabla \mathcal{L}_{m,t}^{(e)}\|_2^2 - \frac{E \eta^2 L_1}{4} \sigma^2.$$

$\square$

**Theorem 2.** *The Aggregator, Verifier, and malicious clients cannot access any sensitive information about benign clients.*

*Proof.* During the secure aggregation, the two servers can obtain plaintext information  $\|\mathbf{C}_{t+1}^k\|$  and  $\text{Sum}_t^k$ , where  $\|\mathbf{C}_{t+1}^k\|$  denotes the norm of trusted update,  $\text{Sum}_t^k$  denotes the sum of aggregation weight of class  $k$ . For non-colluding *Aggregator* and *Verifier*, they cannot get any sensitive information from these plaintext information. In addition, for colluding malicious clients, when there are  $(|\mathcal{S}| - 1)$  malicious clients in PPFPL, they can infer the local prototype about benign client from the encrypted global prototype. However, the real scenario does not exist when there are  $(|\mathcal{S}| - 1)$  malicious clients. Since benign clients receive only global prototypes distributed by *Aggregator*, they cannot deduce information about others. Therefore, neither third-party entities nor malicious clients can derive sensitive information about benign clients.  $\square$

## VII. EXPERIMENTS

In this section, we evaluate the performance of PPFPL in the presence of data poisoning attacks on Non-IID data.

### A. Experimental Settings

1) **Datasets and Models:** Similar to previous works [16] [36] [52], we utilize three public available datasets, namely MNIST, FMNIST, and CIFAR10, to evaluate performance of our PPFPL.

- 1) **MNIST:** This dataset comprises handwritten digits, with a training set of 60,000 samples in 10 classes and a test set of 10,000 samples, each represented as a  $28 \times 28$  gray-scale image.
- 2) **FMNIST:** The FMNIST is a clothing image dataset containing a training set of 60,000 samples in 10 classes and a test set of 10,000 samples, each of which is a  $28 \times 28$  grey-scale image.
- 3) **CIFAR10:** As a color image dataset, CIFAR10 contains a training set of 50,000 samples in 10 classes and a test set of 10,000 samples, with each image measuring  $32 \times 32$  pixels.

Furthermore, we apply Convolution Neural Network (CNN) as local model to both MNIST and FMNIST. For CIFAR-10, we employ ResNet18 as the local model, initialized with pre-trained parameters. These initial parameters have an accuracy of 27.5% on CIFAR10's test set.

2) **Hyper-parameters Settings of FL:** We employ a cross-silo configuration in FL setup. Specifically, we set up 20 clients, each of which uploads local prototypes at each communication round. The number of communication rounds is set to 100, 150, and 150 for MNIST, FMNIST, and CIFAR10, respectively. We configure the local learning rate to  $\eta = 0.01$ , the importance weight to  $\lambda = 1$ , a batch size to 64, and the number of local iterations to  $E = 5$ . Except for special declared, the above default settings are applied. These hyper-parameters are consistent across all clients.

3) **Non-IID Settings:** To simulate the Non-IID data in cross-silo FL, we create class-space heterogeneity among clients, which is common in the cross-silo scenarios. Specifically, large organizations (e.g., hospitals, companies) possess different data classes, and their class distributions may differ significantly, or even be missing some classes altogether. When these organizations participate in federated training, the union of their data classes defines the entire FL classification task. This phenomenon leads to Non-IID data across organizations. The Dirichlet distribution assumes that each client's data is sampled from all classes, meaning each client typically have a positive percentage of every class. However, in cross-silo scenarios, some clients may have no samples from certain classes, which contradicts the assumptions of Dirichlet distribution.

To model the data distribution in cross-silo scenarios, similar to previous works [22] [53], we define *Avg* as the mean number of data classes per client, and *Std* as the standard deviation of these class counts. In our experiments, we fix *Avg* to be 3, 4 or 5, and fix *Std* to be 1 or 2, aiming to create the class-space heterogeneity. Clients are randomly assigned classes, with partial class overlap among them. To visualize the different data distributions, we plot heat maps as shown in Fig. 2.

4) **Setting of Data Poisoning Attacks:** In our experiments, we consider two types of data poisoning attacks: feature

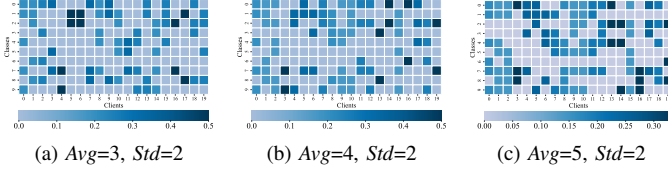


Fig. 2. Heat maps for different data distributions under heterogeneity distribution.

attacks and label attacks. For feature attacks, malicious clients randomly alter their own training data features in a completely randomized manner without following any specific rule. For label attacks, malicious clients alter the labels of their own training data to incorrect labels. All training data of malicious clients are modified. Malicious clients do not dynamically change their behaviors during federated training, and the attack remains consistent throughout the training period. Since the number of malicious clients affects FL performance differently, we set different proportions of malicious clients. Formally,  $Att$  is set as the proportion of malicious clients.

5) *Evaluation Measure*: Our goal is to improve the performance of cross-silo PPFL under poisoned Non-IID data while resisting data poisoning attacks. Therefore, we evaluate the FL performance by testing the average accuracy of benign clients. For experiment comparison, we use FedAvg as the baseline, assuming that FedAvg has not suffered data poisoning attacks. In addition, we compare our PPFL with robust schemes (i.e., Krum [35], Foolsgold [54], and FedDMC [36]) and privacy-preserving robust schemes (i.e., ShieldFL [18], PBFL [16], and AntidoteFL [20]) under the same experiment conditions.

## B. Experimental Results

1) *Visualization of Prototypes*: We visualize the prototypes submitted by clients in PPFL using t-SNE, as shown in Fig. 3. Specifically, we display the distribution of prototypes from clients under feature and label attacks with  $Att = 20\%$  on the CIFAR10 dataset within a single communication round. We observe that the prototypes of malicious clients deviate significantly from those of benign clients, regardless of the features attacks or labels attacks. In addition, we notice that the prototypes submitted by malicious clients are concentrated in a ring area. This is because when malicious clients perform local model training, the features or labels are disrupted, causing the directions of the generated prototypes to spread from the center point to the surrounding areas. Most importantly, we observe a clear difference between the prototypes submitted by benign and malicious clients. This difference is prominent because it is independent of the data distribution. The finding validates the effectiveness of using prototypes to defend against data poisoning attacks. To filter out these malicious prototypes, it is essential to employ a secure aggregation protocol that ensures Byzantine-robust aggregation results. The following is the security evaluation of PPFL.

2) *Security Evaluation*: To evaluate the security of our framework, we test PPFL's performance against feature attacks and label attacks on three datasets under Non-IID setting with  $Avg = 3$  and  $Std = 2$ . Specifically, the proportion

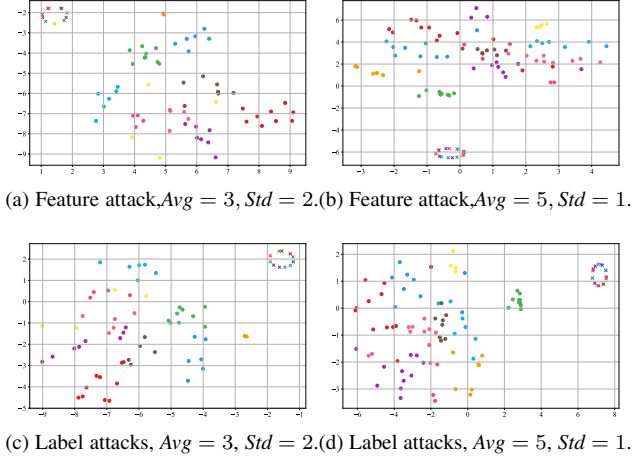


Fig. 3. The t-SNE visualization of prototypes submitted by benign and malicious clients: different colors indicate distinct classes, where “.” denotes prototypes from benign clients, and “x” represents those from malicious clients.

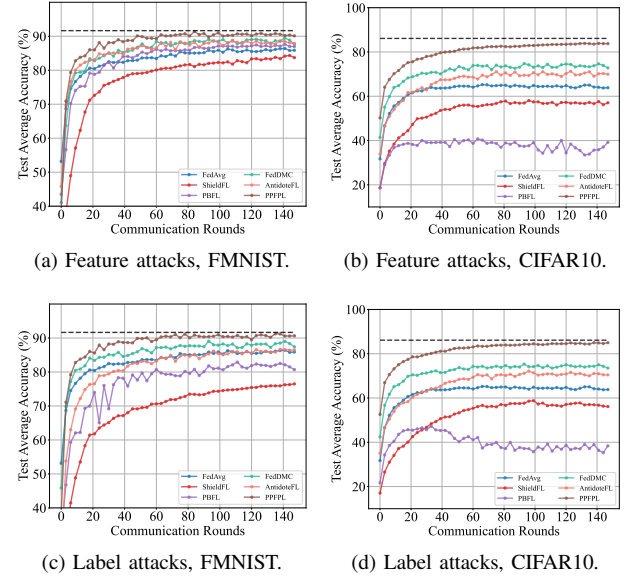


Fig. 4. Test average accuracy comparison between PPFL and existing schemes in poisoned Non-IID data.

of malicious clients is set to  $Att = 20\%$  and the detection threshold of PPFL is configured as  $\chi = 0$ . Furthermore, we compare PPFL with existing schemes (i.e., FedAvg, ShieldFL, PBFL, FedDMC, and AntidoteFL), where the global model learned by FedAvg is not subject to data poisoning attacks.

The experiment results are shown in Fig. 4, where the black dashed line represents the highest accuracy of PPFL without attacks. We observe that the accuracy of ShieldFL and PBFL (under attacks) is severely lower than FedAvg (no attack) in CIFAR10. This indicates that as the dataset becomes more complex, the negative impact of data poisoning attacks on model accuracy becomes more obvious. This is mainly because the complex dataset increases the difficulty of defense, and poisoned Non-IID data degrades

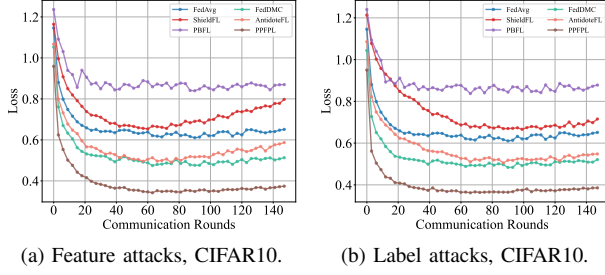


Fig. 5. Loss comparison between PPFPL and existing schemes in poisoned Non-IID data.

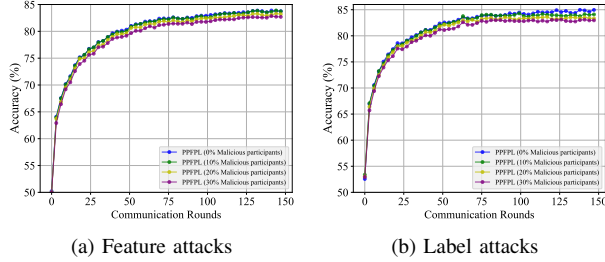


Fig. 6. Stability of PPFPL under CIFAR10 against data poisoning attacks.

the defense performance. Notably, FedDMC and AntidoteFL achieve higher performance compared to FedAvg because they adjust the aggregation weights of the model updates, which mitigates the bias caused by Non-IID data and improves the performance of federated learning. Moreover, PPFPL (under attack) outperforms FedAvg (no attacks), with its accuracy approaching the highest accuracy of PPFPL without attacks when it nears convergence. This demonstrates that PPFPL guarantees the high accuracy of the learned model in the presence of poisoned Non-IID data, which is benefited that the prototype is not affected by tampered data distribution, while the secure aggregation protocol resists malicious prototypes submitted by clients. Thus, our PPFPL overcomes the difficulty confronted by these defense schemes, and improves the FL performance in poisoned Non-IID data.

Additionally, we evaluate the change of loss during training for PPFPL and the compared schemes, as shown in Fig. 5. We notice that the loss of PBFL fluctuates significantly during training process, while PPFPL is relatively smooth. This indicates that data poisoning attacks disrupt the convergence of PBFL, while the convergence of PPFPL is not affected by data poisoning attacks, thus ensuring the accuracy of the model. This is consistent with our Corollary 3. Specifically, PPFPL still satisfies convergence in the presence of data poisoning attacks as long as  $\lambda$ ,  $E$ , and  $\eta$  satisfy a specific relationship among them. Moreover, PPFPL's loss at convergence is lower than other defense schemes under CIFAR10, which can satisfy the design goal of security. Notably, our experiments show that the performance impact of feature attacks and label attacks is similar for PPFPL and other schemes. This indicates that the impact on model performance is similar under poisoned Non-IID data, regardless of the type of data poisoning attacks.

3) *Different Data Distributions for PPFPL*: To further test the security of PPFPL in different data distributions, we evaluate the accuracy of PPFPL against feature attacks under different Non-IID conditions in MNIST, FMNIST and CIFAR10. In addition, we compare the performance of Krum, Foolsgold, ShieldFL, PBFL, FedDMC, and AntidoteFL. The specific experimental results are reported in Table I. Notably, since test average accuracy has fluctuated after each communication round, we select the average of five highest test average accuracies across the communication rounds. From Table I, we can observe that the performance of PPFPL is less affected by changes in data distribution, while other schemes are very susceptible to data distribution. This is attributed to that the client-submitted prototype does not change due to the change in data distribution. In addition, we observe a slight degradation in the performance of PPFPL with  $Att = 30\%$  attacks. This is because the tampered Non-IID data reduces the contribution of effective samples to the model, resulting in a slightly lower performance, which is a reasonable phenomenon. Therefore, our PPFPL improves performance in cross-silo PPFPL under poisoned Non-IID data while resisting data poisoning attacks, which is applicable to deployments in real-world scenarios.

4) *Secure Aggregation Protocol for PPFPL*: To test the usefulness of aggregation protocol, we evaluate the performance of PPFPL with  $\chi$  of -1, 0, 0.2, and 0.5, respectively, where  $\chi = -1$  means that the protocol perform normalization verification and average aggregation, and the data distribution is Non-IID (i.e.,  $Avg = 3, Std = 2$ ). In addition, the  $\mathbf{X}$  in Table II denotes that client-submitted prototypes are unnormalized and aggregated by simple averaging. As shown in Table II, we can observe from  $\mathbf{X}$  that the performance of PPFPL suffers degradation to some extent compared to other settings. The performance degradation stems from the influence of malicious clients' prototypes on the aggregation process, leading to a poisoned global prototype. However, the poisoned global prototype can only affect part of local model training, and cannot affect the minimization of local classification loss. Thus, in PPFPL, the model accuracy of benign clients is less susceptible to the influence of malicious clients. Furthermore, we observe that the presence of detection threshold improves the performance of PPFPL, which indicates that the secure aggregation protocol computes Byzantine-robust aggregation results, which reduces the influence of malicious clients and proves the effectiveness of the secure aggregation protocol. The above observation raises the question: whether PPFPL can maintain high performance in high proportion of attacks? We explore this question in the next experiment.

5) *High Proportion Attacks for PPFPL*: To test the performance of PPFPL under high proportion attacks, we evaluate it with  $Att = 20\%$ ,  $40\%$ ,  $60\%$  and  $80\%$ , respectively. In addition, we set  $\lambda$  as 0.01, 0.1 and 1 respectively, and the data distribution is Non-IID (i.e.,  $Avg = 3, Std = 2$ ). The  $\lambda$  denotes the importance weight of the auxiliary term in loss function, which can be considered as the degree of influence among clients. The experimental results are shown in Fig. 7. We surprisingly observe that PPFPL still has high performance when  $Att$  is  $60\%$  or even  $80\%$ , which indicates that the training of benign clients is not interfered by malicious clients. This is

TABLE I  
TEST AVERAGE ACCURACY (%) ON MNIST, FMNIST AND CIFAR10  
WITH FEATURE ATTACKS.

Dataset	Method	Att %	Std	Test Average Accuracy (%)				
				Avg = 3	Avg = 4	Avg = 5	Avg = 6	Avg = 7
MNIST	Krum	20	2	95.96	96.95	97.01	97.04	<b>97.12</b>
		30	1	95.74	96.61	96.82	<b>96.78</b>	<b>96.92</b>
	Foolsgold	20	2	95.67	94.28	94.88	94.77	95.80
		30	1	96.69	94.03	95.13	95.76	95.39
	PBFL	20	2	96.19	94.82	96.73	95.27	95.75
		30	1	96.47	93.76	94.98	95.21	95.00
	ShieldFL	20	2	96.02	94.74	96.58	95.01	95.49
		30	1	97.78	<b>97.57</b>	96.34	<b>97.10</b>	96.98
	FedDMC	20	2	97.36	96.17	96.26	94.64	95.41
		30	1	95.78	94.15	95.95	96.50	96.75
	AntidoteFL	20	2	95.40	93.62	93.48	94.70	94.62
		30	1	96.91	94.05	95.10	95.64	95.25
	PPFPL	20	2	97.25	94.88	95.69	95.44	95.76
		30	1	97.58	93.79	94.93	95.60	95.81
	FedDMC	20	2	97.08	94.69	95.46	95.73	94.46
		30	1	97.62	97.46	97.16	96.86	96.53
	AntidoteFL	20	2	97.53	97.32	97.04	96.73	96.39
		30	1	97.62	96.98	96.88	96.46	96.17
FMNIST	Krum	20	2	97.43	96.58	96.34	96.26	94.33
		30	1	97.40	97.09	96.73	96.34	96.30
	Foolsgold	20	2	97.31	97.18	96.85	95.45	96.30
		30	1	97.35	96.39	96.42	96.06	96.20
	PBFL	20	2	97.08	94.69	95.46	95.73	94.46
		30	1	<b>97.87</b>	97.53	<b>97.35</b>	97.08	96.89
	ShieldFL	20	2	<b>97.74</b>	<b>97.49</b>	<b>97.43</b>	<b>96.82</b>	<b>96.56</b>
		30	1	<b>97.85</b>	<b>97.04</b>	<b>97.02</b>	<b>96.52</b>	<b>96.37</b>
	FedDMC	20	2	<b>97.52</b>	<b>96.92</b>	<b>96.70</b>	<b>96.50</b>	<b>96.48</b>
		30	1	84.24	84.80	86.03	86.52	87.35
	AntidoteFL	20	2	85.02	83.64	86.82	84.75	86.08
		30	1	83.72	84.38	85.49	85.12	86.79
	PPFPL	20	2	84.62	82.73	85.73	82.86	84.09
		30	1	84.83	84.75	84.04	83.55	82.62
	Foolsgold	20	2	82.49	83.88	85.31	81.75	82.24
		30	1	84.06	84.01	83.50	82.70	82.04
	PBFL	20	2	81.86	83.43	84.98	81.19	82.68
CIFAR10	Krum	20	2	87.01	80.37	76.93	74.26	72.10
		30	1	87.42	76.31	74.47	72.99	72.43
	Foolsgold	20	2	86.92	75.45	73.06	73.70	72.84
		30	1	79.34	72.68	72.81	70.57	70.49
	PBFL	20	2	87.01	78.90	78.06	70.90	70.26
		30	1	76.47	77.89	70.96	67.47	66.80
	ShieldFL	20	2	86.24	78.46	77.51	68.81	68.81
		30	1	75.81	77.35	70.57	66.42	65.46
	FedDMC	20	2	90.60	88.21	87.03	86.40	86.11
		30	1	89.53	88.70	87.27	87.20	87.13
	AntidoteFL	20	2	89.73	88.03	86.38	86.70	86.14
		30	1	89.40	87.52	86.23	86.40	86.12
	PPFPL	20	2	89.13	87.20	87.03	86.40	86.11
		30	1	88.72	86.13	85.34	85.16	86.48
	Foolsgold	20	2	87.25	86.24	85.13	84.10	84.25
		30	1	87.10	86.61	85.10	84.39	84.90
	PBFL	20	2	<b>91.38</b>	<b>90.18</b>	<b>89.27</b>	<b>88.56</b>	<b>88.13</b>
		30	1	<b>90.48</b>	<b>89.63</b>	<b>88.45</b>	<b>88.79</b>	<b>88.20</b>
CIFAR10	Krum	20	2	<b>90.97</b>	<b>90.08</b>	<b>88.93</b>	<b>88.33</b>	<b>88.14</b>
		30	1	<b>90.40</b>	<b>88.62</b>	<b>87.74</b>	<b>88.41</b>	<b>87.97</b>
	Foolsgold	20	2	62.91	61.24	68.19	68.87	69.22
		30	1	57.90	57.94	68.33	68.65	68.79
	PBFL	20	2	60.10	60.73	66.36	68.70	69.01
		30	1	56.67	57.29	67.03	68.49	68.51
	ShieldFL	20	2	60.91	59.24	66.19	66.45	66.52
		30	1	56.90	55.94	66.33	66.62	66.70
	FedDMC	20	2	60.37	58.68	65.64	66.26	66.44
		30	1	56.17	55.09	65.85	66.40	66.41
	AntidoteFL	20	2	38.06	39.18	41.81	42.42	42.75
		30	1	39.46	40.54	41.30	42.12	42.76
	PPFPL	20	2	37.18	39.02	41.39	42.32	42.41
		30	1	37.80	37.52	41.08	41.96	42.67
	Foolsgold	20	2	61.62	61.94	68.31	69.53	68.66
		30	1	57.84	57.26	66.14	67.43	68.62
	PBFL	20	2	60.94	61.25	67.50	67.01	68.24
		30	1	57.10	56.76	65.47	66.42	67.69
CIFAR10	Krum	20	2	75.28	74.16	74.37	73.86	<b>73.50</b>
		30	1	72.66	72.40	72.37	72.06	71.58
	Foolsgold	20	2	72.67	72.48	72.11	71.85	70.78
		30	1	72.66	72.27	71.19	72.19	70.65
	PBFL	20	2	70.86	70.40	70.19	69.84	69.75
		30	1	71.49	71.61	70.43	71.24	69.20
	ShieldFL	20	2	69.82	68.70	68.42	68.83	68.17
		30	1	<b>83.41</b>	<b>80.95</b>	<b>77.82</b>	<b>74.76</b>	71.35
	FedDMC	20	2	83.44	83.24	77.19	74.64	71.60
		30	1	<b>83.31</b>	<b>81.03</b>	<b>77.18</b>	<b>74.53</b>	71.15
	AntidoteFL	20	2	<b>83.16</b>	<b>82.37</b>	<b>77.47</b>	<b>74.62</b>	71.19
		30	1	83.16	82.37	77.47	74.62	71.19

TABLE II  
TEST AVERAGE ACCURACY (%) ON MNIST, FMNIST AND CIFAR10  
WITH DIFFERENT  $\chi$  ON FEATURE ATTACKS.

Datasets	Att	$\chi = -1$	$\chi = 0$	$\chi = 0.2$	$\chi = 0.5$	$\chi$
MNIST	10%	96.23	97.86	97.62	98.16	95.73
	20%	96.10	97.20	97.55	97.03	94.35
	30%	95.21	97.10	97.47	97.82	94.20
	40%	94.54	96.75	96.51	96.48	93.14
FMNIST	10%	88.37	90.68	90.23	90.78	86.14
	20%	88.20	90.28	90.36	90.48	86.12
	30%	88.03	90.14	90.06	90.16	85.71
	40%	87.62	90.23	90.41	90.04	85.29
CIFAR10	10%	81.66	83.59	83.10	83.24	80.97
	20%	81.61	83.57	83.67	83.31	79.53
	30%	81.38	83.45	83.35	83.21	78.08
	40%	80.74	83.05	83.27	82.94	78.00

because the benign client does not rely solely on information distributed by two servers in federated prototype learning, but relies heavily on its local training data. Furthermore, we observe that when  $Att$  is 20% or 40%, the accuracy increases slightly with the growth of  $\lambda$  in the three datasets. On the contrary, when  $Att$  is 60% or 80%, the accuracy

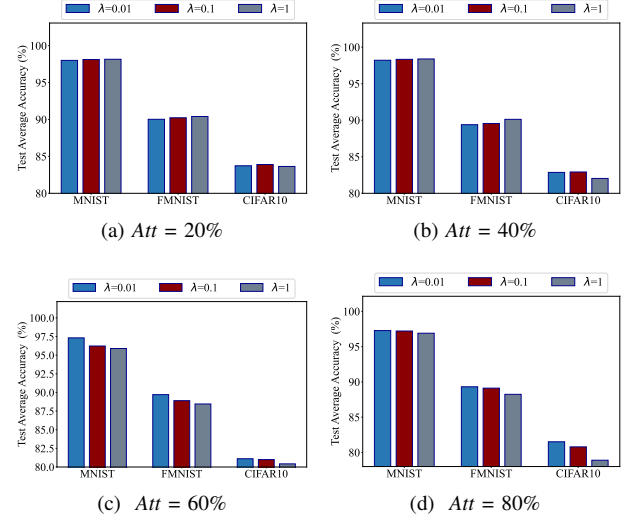


Fig. 7. Test average accuracy of different  $\lambda$  with different proportions  $Att$  with feature attacks.

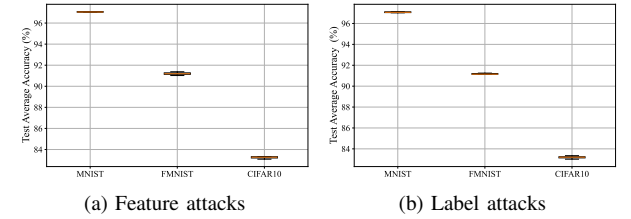


Fig. 8. Stability of PPFPL under MNIST, FMNIST, and CIFAR10.

tends to decrease with the increase of  $\lambda$ . This is because the larger  $\lambda$  strengthens the collaboration among clients, but makes PPFPL more vulnerable to data poisoning attacks from malicious clients. Conversely, the smaller value of  $\lambda$  weakens collaboration among clients, but increases resistance to data poisoning attacks. Therefore, PPFPL can appropriately adjust the size of  $\lambda$  according to actual conditions.

6) *Stability of PPFPL*: It is observed from Fig. 4 and 5 that the performance of PPFPL exhibits some fluctuations. Therefore, it is important to evaluate the stability of PPFPL over multiple randomized experiments. To verify the stability of PPFPL, we conduct experiments using the MNIST, FMNIST, and CIFAR10 datasets, with 20% of clients being malicious. The data distribution is Non-IID (i.e.,  $Avg = 3, Std = 2$ ). Each experiment is repeated 10 times. The utilization of boxplots in Fig. 8 provides a clear visualization of the stability of PPFPL. The results show that PPFPL's performance fluctuates less and remains stable against data poisoning attacks. The stability of PPFPL proves its reliability in real-world scenarios.

7) *Scalability of PPFPL*: Federated learning is often deployed with an uncertain number of clients, and scalability directly determines whether PPFPL can maintain stable performance in environments with different numbers of clients. To evaluate the scalability of PPFPL, we conducted experiments on the MNIST, FMNIST, and CIFAR10 datasets with 20% malicious clients, and the number of clients set to 20, 25, 30, 35, and 40. The data distribution is Non-IID



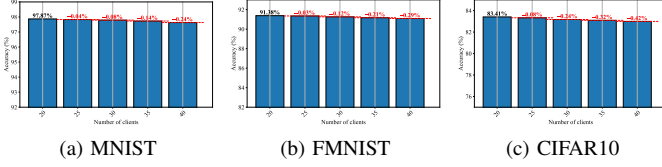


Fig. 9. Scalability of PPFPL against data poisoning attacks over the MNIST, FMNIST, and CIFAR10.

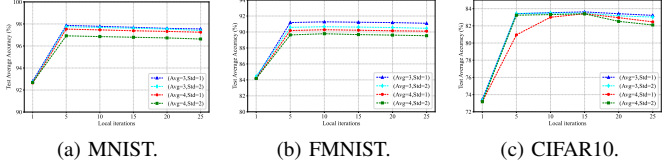


Fig. 10. The test average accuracy on three datasets with different number of local iterations under feature attacks.

(i.e.,  $Avg = 3, Std = 1$ ). Fig. 9 shows the scalability of PPFPL against data poisoning attacks. It is observed that the performance of PPFPL drops by 0.24% on MNIST and 0.42% on CIFAR10 when the number of participants is increased by 100%, which is normal in federated learning. Thus, PPFPL shows excellent scalability against data poisoning attacks with data heterogeneity.

8) *Impact of Local Iterations*: We investigate the effect of the number of local iterations on the test average accuracy for PPFPL. We conduct experiments on MNIST, FMNIST, and CIFAR10 datasets, where 20% of malicious clients launched feature attacks. The number of local iterations are 1, 5, 10, 15, 20 and 25. The results are shown in Fig. 10. We observe that when the number of local iterations is 1, the changes in the local model are very small, resulting in slow training and relatively low accuracy for the same number of communication rounds. When the number of local iterations is 5, PPFPL has the highest test average accuracy on the MNIST dataset. However, on CIFAR10, the optimal number of local iterations should be set to 15. In addition, when the number of local iterations is too high, the test average accuracy decreases, which is due to the overfitting of the local model.

9) *Efficiency Evaluation*: To evaluate the efficiency of PPFPL, we measure the number of parameters submitted by clients, as shown in Fig. 11. We can observe that since the number of parameters submitted by PBFL and ShieldFL depends on the model architecture, their clients submit the same amount of parameters. Furthermore, the number of parameters submitted by clients in PPFPL is much lower than in PBFL under the same model architecture. This is because the number of prototype parameters in PPFPL depends on the compression of the feature extractor's output, rather than the model architecture. Thus, PPFPL reduces the number of parameters submitted to two servers, thereby reducing the privacy computation overheads and communication overheads.

In addition, ciphertext operations are the primary factor affecting the efficiency of our framework. We evaluate the time cost of PPFPL, PBFL, and ShieldFL on ciphertext operations. Note that PBFL is a federated learning scheme

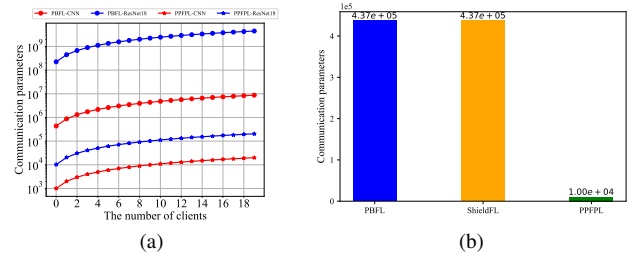


Fig. 11. Communication parameters. (a) The number of parameters submitted by clients under different local models. (b) The number of parameters submitted by client using CNN model in one round under different scheme.

TABLE III  
THE COST TIME OF CIPHERTEXT OPERATION USING CNN MODEL UNDER PBFL, SHIELDFL, AND PPFPL.

Operation	PBFL	ShieldFL	PPFPL
Encrypt	1.72s	1.42s	0.62s
Decrypt	1.35s	1.19s	0.40s

based on CKKS, while ShieldFL is built upon the two-door HE. For each client, we use the time spent on encryption and decryption for each iteration as a metric. As shown in Table III, PPFPL has advantages in encryption and decryption compared to PBFL and ShieldFL. This is because the number of prototype parameters submitted by clients is lower in PPFPL, which greatly improves the computational efficiency and reduces the computational cost.

### C. Complexity Analysis

We analyze the computational overload and communication overload for each client in PPFPL and compared it with similar schemes [16] [18] [15]. The results are shown in Table IV. The computational overload for the clients in PPFPL comprises three components: local model training, prototype generation, and encryption. Formally, the computational overhead is expressed as  $\mathcal{O}(T_{tr}) + \mathcal{O}(T_{pro}) + \mathcal{O}(pT_{ch})$ , where  $p$  denotes the prototype parameters,  $T_{ch}$  denotes the time overload of encryption,  $T_{tr}$  denotes the time overhead of local model training, and  $T_{pro}$  denotes the time overhead of prototype generation. Notably, the overhead of prototype generation is significantly lower than that of local model training, i.e.,  $T_{tr} \gg T_{pro}$ . Other similar schemes [16] [18] [15] adopt homomorphic encryption on gradients, their encryption overhead is  $\mathcal{O}(gT_{ch})$ , where  $g$  denotes the gradient parameters. Since  $g > p$ , the overload satisfies  $\mathcal{O}(gT_{ch}) > \mathcal{O}(pT_{ch})$ . Hence, the relationship  $\mathcal{O}(T_{tr}) + \mathcal{O}(gT_{mul}) + \mathcal{O}(gT_{ch}) > \mathcal{O}(T_{tr}) + \mathcal{O}(gT_{ch}) > \mathcal{O}(T_{tr}) + \mathcal{O}(T_{pro}) + \mathcal{O}(pT_{ch})$  holds. Consequently, PPFPL imposes a reasonable computational overhead on clients.

TABLE IV  
COMPUTATION OVERLOAD AND COMMUNICATION OVERLOAD OF CLIENT.

Scheme	Computation Overload	Communication Overload
PEFL [15]	$\mathcal{O}(T_{tr}) + \mathcal{O}(gT_{ch})$	$\mathcal{O}(gP_h)$
ShieldFL [18]	$\mathcal{O}(T_{tr}) + \mathcal{O}(gT_{mul}) + \mathcal{O}(gT_{ch})$	$\mathcal{O}(gP_h)$
PBFL [16]	$\mathcal{O}(T_{tr}) + \mathcal{O}(gT_{ch})$	$\mathcal{O}(gP_h)$
PPFPL	$\mathcal{O}(T_{tr}) + \mathcal{O}(T_{pro}) + \mathcal{O}(pT_{ch})$	$\mathcal{O}(nP_h)$

In addition, the client communication overhead is  $\mathcal{O}(nP_h)$  in PPFL, where  $P_h$  denotes the communication complexity of a number. Compared with [16] [18] [15], the relationship  $\mathcal{O}(gP_h) > \mathcal{O}(pP_h)$  holds.

## VIII. CONCLUDES

In this paper, we propose PPFL, a privacy-preserving federated prototype learning framework, which improves performance while resisting data poisoning attacks in poisoned Non-IID data. Our work is the first to introduce prototype learning into PPFL to address privacy threats and data poisoning attacks in across-silo FL. As for how to implement lightweight privacy-preserving FL to resist data poisoning attacks on Non-IID data, we leave them to future exploration.

## REFERENCES

- [1] R. Zhang, H. Li, L. Tian, M. Hao, and Y. Zhang, "Vertical federated learning across heterogeneous regions for industry 4.0," *IEEE Transactions on Industrial Informatics*, vol. 20, no. 8, pp. 10 145–10 155, 2024.
- [2] S. Kalloori and A. Srivastava, "Towards cross-silo federated learning for corporate organizations," *Knowledge-Based Systems*, vol. 289, p. 111501, 2024.
- [3] Y. Jin, Y. Liu, K. Chen, and Q. Yang, "Federated learning without full labels: A survey," *arXiv preprint arXiv:2303.14453*, 2023.
- [4] B. Rao, J. Zhang, D. Wu, C. Zhu, X. Sun, and B. Chen, "Privacy inference attack and defense in centralized and federated learning: A comprehensive survey," *IEEE Transactions on Artificial Intelligence*, vol. 6, no. 2, pp. 333–353, 2025.
- [5] Y. Qin, X. Zheng, Q. Ma, G. Liao, and X. Chen, "Participation-dependent privacy preservation in cross-silo federated learning," *IEEE Transactions on Services Computing*, vol. 18, no. 1, pp. 342–356, 2025.
- [6] G. Huang, Q. Wu, P. Sun, Q. Ma, and X. Chen, "Collaboration in federated learning with differential privacy: A stackelberg game analysis," *IEEE Transactions on Parallel and Distributed Systems*, vol. 35, no. 3, pp. 455–469, 2024.
- [7] J. Ling, J. Zheng, and J. Chen, "Efficient federated learning privacy preservation method with heterogeneous differential privacy," *Computers & Security*, vol. 139, p. 103715, 2024.
- [8] Y. Li, N. Yan, J. Chen, X. Wang, J. Hong, K. He, W. Wang, and B. Li, "Fedphe: A secure and efficient federated learning via packed homomorphic encryption," *IEEE Transactions on Dependable and Secure Computing*, pp. 1–16, 2025.
- [9] A. Catalfamo, L. Carnevale, M. Garofalo, and M. Villari, "Flower full-compliant implementation of federated learning with homomorphic encryption," in *2024 IEEE Symposium on Computers and Communications (ISCC)*, 2024, pp. 1–5.
- [10] K. Kumar, C. Mohan, and L. Cenkaramaddi, "The impact of adversarial attacks on federated learning: A survey," *IEEE Transactions on Pattern Analysis and Machine Intelligence*, vol. 46, no. 5, pp. 2672–2691, 2024.
- [11] J. Fan, Q. Yan, M. Li, G. Qu, and Y. Xiao, "A survey on data poisoning attacks and defenses," in *Proceedings of IEEE International Conference on Data Science in Cyberspace*, 2022, pp. 48–55.
- [12] J. Zhang, C. Zhu, C. Ge, C. Ma, Y. Zhao, X. Sun, and B. Chen, "Bad-cleaner: Defending backdoor attacks in federated learning via attention-based multi-teacher distillation," *IEEE Transactions on Dependable and Secure Computing*, vol. 21, no. 5, pp. 4559–4573, 2024.
- [13] C. Zhu, J. Zhang, X. Sun, B. Chen, and W. Meng, "Adfl: Defending backdoor attacks in federated learning via adversarial distillation," *Computers Security*, vol. 132, p. 103366, 2023.
- [14] M. Hao, H. Li, G. Xu, H. Chen, and T. Zhang, "Efficient, private and robust federated learning," in *Proceedings of the Annual Computer Security Applications Conference*, 2021, pp. 45–60.
- [15] X. Liu, H. Li, G. Xu, Z. Chen, X. Huang, and R. Lu, "Privacy-enhanced federated learning against poisoning adversaries," *IEEE Transactions on Information Forensics and Security*, vol. 16, pp. 4574–4588, 2021.
- [16] Y. Miao, Z. Liu, H. Li, K. Choo, and R. H. Deng, "Privacy-preserving byzantine-robust federated learning via blockchain systems," *IEEE Transactions on Information Forensics and Security*, vol. 17, pp. 2848–2861, 2022.
- [17] X. Li, X. Yang, Z. Zhou, and R. Lu, "Efficiently achieving privacy preservation and poisoning attack resistance in federated learning," *IEEE Transactions on Information Forensics and Security*, vol. 19, pp. 4358–4373, 2024.
- [18] Z. Ma, J. Ma, Y. Miao, Y. Li, and R. H. Deng, "Shieldfl: Mitigating model poisoning attacks in privacy-preserving federated learning," *IEEE Transactions on Information Forensics and Security*, vol. 17, pp. 1639–1654, 2022.
- [19] X. Chen, H. Yu, X. Jia, and X. Yu, "Apfed: Anti-poisoning attacks in privacy-preserving heterogeneous federated learning," *IEEE Transactions on Information Forensics and Security*, vol. 18, pp. 5749–5761, 2023.
- [20] Y. Liu, H. Zhang, M. Wang, Q. Xie, and Z. Sun, "Antidoteff: Enhancing defense against poisoning attacks in federated learning," *Computer Networks*, p. 111427, 2025.
- [21] H.-M. Yang, X.-Y. Zhang, F. Yin, and C.-L. Liu, "Robust classification with convolutional prototype learning," in *Proceedings of the IEEE conference on computer vision and pattern recognition*, 2018, pp. 3474–3482.
- [22] Y. Tan, G. Long, L. Liu *et al.*, "Fedproto: Federated prototype learning across heterogeneous clients," in *Proceedings of the AAAI Conference on Artificial Intelligence*, vol. 36, no. 8, 2022, pp. 8432–8440.
- [23] W. Huang, M. Ye, Z. Shi, H. Li, and B. Du, "Rethinking federated learning with domain shift: A prototype view," in *Proceedings of Conference on Computer Vision and Pattern Recognition*, 2023, pp. 16312–16322.
- [24] S. Guo, H. Wang, and X. Geng, "Dynamic heterogeneous federated learning with multi-level prototypes," *Pattern Recognition*, vol. 153, p. 110542, 2024.
- [25] X. Mu, Y. Shen, K. Cheng *et al.*, "Fedproc: Prototypical contrastive federated learning on non-iid data," *Future Generation Computer Systems*, vol. 143, pp. 93–104, 2023.
- [26] S. Truex, L. Liu, K.-H. Chow, M. E. Gursoy, and W. Wei, "Ldp-fed: federated learning with local differential privacy," in *Proceedings of the ACM International Workshop on Edge Systems, Analytics and Networking*, 2020, p. 61–66.
- [27] Y. Zhao, J. Zhao, M. Yang, T. Wang, N. Wang, L. Lyu, D. Niyato, and K. Y. Lam, "Local differential privacy-based federated learning for internet of things," *IEEE Internet of Things Journal*, vol. 8, no. 11, pp. 8836–8853, 2020.
- [28] K. Wei, J. Li, M. Ding, C. Ma, H. Su, B. Zhang, and H. V. Poor, "User-level privacy-preserving federated learning: Analysis and performance optimization," *IEEE Transactions on Mobile Computing*, vol. 21, no. 9, pp. 3388–3401, 2022.
- [29] C. Wang, X. Wu, G. Liu, T. Deng, K. Peng, and S. Wan, "Safeguarding cross-silo federated learning with local differential privacy," *Digital Communications and Networks*, vol. 8, no. 4, pp. 446–454, 2022.
- [30] H. Fang and Q. Qian, "Privacy preserving machine learning with homomorphic encryption and federated learning," *Future Internet*, vol. 13, no. 4, 2021.
- [31] P. Paillier, "Public-key cryptosystems based on composite degree residuosity classes," in *Proceedings of International conference on the theory and applications of cryptographic techniques*, 1999, pp. 223–238.
- [32] J. Ma, S. A. Naas, S. Sigg, and X. Lyu, "Privacy-preserving federated learning based on multi-key homomorphic encryption," *International Journal of Intelligent Systems*, vol. 37, no. 9, pp. 5880–5901, 2022.
- [33] B. Li and D. Micciancio, "On the security of homomorphic encryption on approximate numbers," in *Proceedings of Annual International Conference on the Theory and Applications of Cryptographic Techniques*, 2021, pp. 648–677.
- [34] V. Tolpegin, S. Truex, M. E. Gursoy, and L. Liu, "Data poisoning attacks against federated learning systems," in *Proceedings of Computer Security ESORICS*, 2020, pp. 480–501.
- [35] P. Blanchard, E. M. El Mhamdi, R. Guerraoui, and J. Stainer, "Machine learning with adversaries: Byzantine tolerant gradient descent," *Advances in neural information processing systems*, vol. 30, 2017.
- [36] X. Mu, K. Cheng, Y. Shen, X. Li, Z. Chang, T. Zhang, and X. Ma, "Feddmc: Efficient and robust federated learning via detecting malicious clients," *IEEE Transactions on Dependable and Secure Computing*, vol. 21, no. 6, pp. 5259–5274, 2024.
- [37] X. Zhang, Q. Liu, Z. Ba, Y. Hong, T. Zheng, F. Lin, L. Lu, and K. Ren, "Fltrac: Accurate poisoning attack provenance in federated learning," *IEEE Transactions on Information Forensics and Security*, vol. 19, pp. 9534–9549, 2024.
- [38] R. Doku and D. B. Rawat, "Mitigating data poisoning attacks on a federated learning-edge computing network," in *Proceedings of IEEE*

- Annual Consumer Communications Networking Conference*, 2021, pp. 1–6.
- [39] T. Li, A. Sahu, M. Zaheer, M. Sanjabi, A. Talwalkar, and V. Smith, “Federated optimization in heterogeneous networks,” in *Proceedings of Machine learning and systems*, vol. 2, 2020, pp. 429–450.
  - [40] D. Acar, Y. Zhao, R. Navarro, M. Mattina, P. Whatmough, and V. Saligrama, “Federated learning based on dynamic regularization,” *Proceedings of International Conference on Learning Representations*, 2021.
  - [41] J. Zhang, Z. Li, B. Li *et al.*, “Federated learning with label distribution skew via logits calibration,” in *Proceedings of International Conference on Machine Learning*, 2022, pp. 26 311–26 329.
  - [42] F. Zhu, X. Y. Zhang, C. Wang, F. Yin, and C. L. Liu, “Prototype augmentation and self-supervision for incremental learning,” in *Proceedings of the IEEE/CVF Conference on Computer Vision and Pattern Recognition*, June 2021, pp. 5871–5880.
  - [43] M. J. Wiener, “Cryptanalysis of short rsa secret exponents,” *IEEE Transactions on Information theory*, vol. 36, no. 3, pp. 553–558, 1990.
  - [44] Y. Tsionis and M. Yung, “On the security of elgamal based encryption,” in *International Workshop on Public Key Cryptography*, 1998, pp. 117–134.
  - [45] S. Akherati and X. Zhang, “Low-complexity ciphertext multiplication for ckks homomorphic encryption,” *IEEE Transactions on Circuits and Systems II: Express Briefs*, vol. 71, no. 3, pp. 1396–1400, 2024.
  - [46] J. Cheon, A. Kim, M. Kim, and Y. Song, “Homomorphic encryption for arithmetic of approximate numbers,” in *Proceedings of International Conference on the Theory and Applications of Cryptology and Information Security*, 2017, pp. 409–437.
  - [47] X. Shen, Y. Liu, F. Li, and C. Li, “Privacy-preserving federated learning against label-flipping attacks on non-iid data,” *IEEE Internet of Things Journal*, vol. 11, no. 1, pp. 1241–1255, 2024.
  - [48] G. Qi, Y. Chen, X. Mao, B. Hui, X. Li, R. Zhang, and H. Xue, “Model inversion attack via dynamic memory learning,” in *Proceedings of International Conference on Multimedia*, 2023, p. 5614–5622.
  - [49] J. Cheon, D. Kim, D. Kim, H. Lee, and K. Lee, “Numerical method for comparison on homomorphically encrypted numbers,” in *Proceedings of Numerical method for comparison on homomorphically encrypted number*, 2019, pp. 415–445.
  - [50] A. Kim, A. Papadimitriou, and Y. Polyakov, “Approximate homomorphic encryption with reduced approximation error,” in *Proceedings of Cryptographers Track at the RSA Conference*, 2022, pp. 120–144.
  - [51] J. Wang, Q. Liu, H. Liang, G. Joshi, and H. V. Poor, “Tackling the objective inconsistency problem in heterogeneous federated optimization,” *Advances in neural information processing systems*, vol. 33, pp. 7611–7623, 2020.
  - [52] J. Zhang, C. Zhu, X. Sun, C. Ge, B. Chen, W. Susilo, and S. Yu, “Flpurifier: Backdoor defense in federated learning via decoupled contrastive training,” *IEEE Transactions on Information Forensics and Security*, vol. 19, pp. 4752–4766, 2024.
  - [53] B. Yan, H. Zhang, M. Xu, D. Yu, and X. Cheng, “Fedrfq: Prototype-based federated learning with reduced redundancy, minimal failure, and enhanced quality,” *IEEE Transactions on Computers*, vol. 73, no. 4, pp. 1086–1098, 2024.
  - [54] C. Fung, C. J. Yoon, and I. Beschastnikh, “The limitations of federated learning in sybil settings,” in *23rd International symposium on research in attacks, intrusions and defenses*, 2020, pp. 301–316.